The Aeronautical Journal (2026), 1–32
doi:10.1017/aer.2026.10264

ROYAL AERONAUTICAL SOCIETY

RESEARCH ARTICLE

Optimum fuel use for turbofan-powered aircraft in a completely general atmosphere with an improved range equation

D.I.A. Poll[1] and U. Schumann[2]

[1]Emeritus Professor of Aerospace Engineering, Cranfield University, Bedford, UK
[2]Deutsches Zentrum für Luft- und Raumfahrt, Institut für Physik der Atmosphäre, Oberpfaffenhofen, Germany
Corresponding author: D.I.A. Poll; Email: d.i.a.poll@cranfield.ac.uk

Received: 21 July 2026 UTC; **Revised:** 1 October 2026 UTC; **Accepted:** 1 October 2026 UTC

Keywords: fuel use; general atmosphere; operational optimum; range; turbofan

Abstract

Fuel requirement is one of the most important issues in aircraft performance. For an aircraft of a given mass, flying in an atmosphere where temperature is a monotonically decreasing function of pressure, there is one Mach number and flight level (FL) pair for which the specific air range (SAR), i.e. the distance travelled through the air per unit mass of fuel consumed, is a maximum. Specific air range is directly proportional to the range parameter, which is the product of the overall engine efficiency and the airframe lift-to-drag ratio. During the aircraft design process, the optimum value of the range parameter is fixed at a specific 'design' mass in a specific 'design' atmosphere. This 'design optimum' condition is a characteristic of the aircraft and engine combination, occurring at a particular Mach number and flight level pair. However, in routine operations, the aircraft mass and the atmospheric characteristics will rarely, if ever, coincide with the design conditions. Consequently, in general, the operational optimum Mach number and flight level pair will not be the same as that at the design optimum. The primary purpose of this analysis is to find the general relationship between the operational and the design conditions. In performance calculations, it is often assumed that, if the Mach number and lift coefficient are constant, the range parameter is also constant. This leads to the well-known 'cruise climb' trajectory for 'maximum' range and, for the whole flight, the classical Breguet range equation for the required trip fuel. However, to maintain a constant lift coefficient, the aircraft must climb as mass reduces and, depending upon the relationship between temperature and pressure in the atmosphere, its Reynolds number changes. It is shown that these Reynolds number changes can alter the range parameter by several percent as the flight progresses, and the standard Breguet equation may produce significant errors in the trip fuel estimation. Therefore, a completely general formulation of the range equation is presented. The well-documented, open-source, Poll-Schumann aircraft performance model is used to provide data for a wide range of operating conditions. Tabulated coefficients are provided to allow operational estimates to be made for 71 aircraft types and variants. These values are best estimates based upon information available in the public domain.

Nomenclature

A	constant coefficient – Equations (55) and (57)
a	coefficient in Equation (21)
a_∞	ambient sound speed $= (\gamma \Re T_\infty)^{1/2}$ (m/s)
B	constant coefficient – Equation (64)
b	coefficient in Equation (21)
C	constant coefficient – Equation (67)
C_D	airframe drag coefficient $= D/(q_\infty S_{ref})$
C_F	mean skin friction coefficient – Equation (21)
C_L	overall lift coefficient $= L/(q_\infty S_{ref})$

© The Author(s), 2026. Published by Cambridge University Press on behalf of Royal Aeronautical Society. This is an Open Access article, distributed under the terms of the Creative Commons Attribution licence (https://creativecommons.org/licenses/by/4.0/), which permits unrestricted re-use, distribution and reproduction, provided the original article is properly cited.
https://doi.org/10.1017/aer.2026.10264 Published online by Cambridge University Press

C_P	specific heat at constant pressure for air (1005 J/(kg K))
C_T	aircraft total net thrust coefficient $= n.F_n/(q_\infty S_{ref})$
D	aircraft total drag force (N)
E	constant coefficient – Equation (70)
F	constant coefficient – Equation (73)
FL	flight level
F_n	net installed thrust per engine (N)
f	correction function – Equation (35)
G	constant coefficient – Equation (76)
H	constant coefficient – Equation (81)
h	geopotential altitude (m)
L	aircraft lift force (N)
LCV	lower calorific value of fuel ($\approx 43 \times 10^6$ J/kg for kerosene)
L/D	lift-to-drag ratio
LR	non-dimensional atmospheric temperature lapse rate – Equation (A18)
L_h	rate of change of temperature with geopotential altitude K/m
M_∞	flight Mach number $= V_\infty / a_\infty$
$MTOM$	maximum permitted take-off mass (kg)
m	instantaneous total aircraft mass (kg)
m_f	instantaneous fuel mass (kg)
n	number of engines
p	static pressure (Pa)
q_∞	freestream dynamic pressure $= 0.5\rho_\infty (V_\infty)^2 = 0.5\gamma p_\infty (M_\infty)^2$ (Pa)
R^{ac}	characteristic aircraft Reynolds number
R_G	total ground distance travelled (m)
$\Re$	gas constant for air (287.05 J/(kg K))
S_{ref}	aerodynamic reference wing area (Airbus definition) (m^2)
S	distance travelled through the air (m)
S_G	distance travelled over the ground (m)
T	static temperature (K)
V_w	tailwind (m/s)
V_∞	true air speed (m/s)
X	non-dimensional ground distance - Equation (100)
β	dummy variable – Equation (35)
γ	ratio of specific heats for air (=1.4)
δ	dummy variable – Equation (35)
η_o	propulsion system overall efficiency - Equation (1)
η_1, η_2	constants in Equation (13)
μ	dynamic viscosity (Pa.s)
ξ_{1-4}	constant coefficients – Equations (42), (39), (40) and (41)
ρ	air density $= p/(\Re T)$ (kg/m^3)
τ	constant coefficient
ϕ	atmospheric temperature function - Equation (A1)
ψ_{1-6}	constant coefficients - Equations (24) to (27), (49) and (50)

Superscripts

ac	whole aircraft value
M	at constant Mach number
P	at constant pressure or constant flight level

Subscripts

B	best, or local maximum, value
DO	at the design optimum conditions

https://doi.org/10.1017/aer.2026.10264 Published online by Cambridge University Press

ISA	in the International Standard Atmosphere
OO	operational optimum value
ref	reference
∞	flight, or freestream, value

1.0 Introduction

Aviation's impact upon the environment continues to be an area of concern and, consequently, an area for continuing research. One particularly important parameter is the specific air range (SAR), which is the distance travelled through the air per unit mass of fuel consumed. Whilst kerosene remains the principal fuel for aviation, SAR determines the amount of carbon dioxide that an aircraft releases into the atmosphere.

In general, SAR depends upon the instantaneous mass of the aircraft, the Mach number, the flight level (FL) and the variation of temperature with pressure in the atmosphere. Importantly, for an aircraft of given mass flying through a specified atmosphere, there is a single Mach number and FL pair at which the SAR is a maximum. This is termed the 'operational' optimum. Knowledge of the conditions for the operational optima is important if, for example, flight trajectories with minimum environmental impact are to be identified, or the efficiency of airline operations is to be judged.

When an aircraft is designed, its optimum cruise performance is determined at a specific mass for flight in a specific atmosphere, usually the monotonically decreasing, International Standard Atmosphere (ISA) [1]. Consequently, this design optimum condition is a fixed characteristic of the particular airframe and engine combination. This has been discussed at length in previous work by Poll and Schumann [2–4] and estimates of the design optimum conditions have been presented. A data set that originally contained 53 aircraft types and variants had been gradually refined, improved and extended with the latest values for 71 aircraft types being listed in Poll and Schumann [4]. The issue of the operational optima for aircraft of any mass flying through a completely general atmosphere was discussed briefly in Reference [2], and initial suggestions for their estimation were presented. This study shows that this approach produces results that are not sufficiently accurate for general use, but, with only slight modifications, very accurate values can be obtained.

Integration of the SAR over the full air distance travelled yields the total fuel needed for the flight, i.e. the trip fuel. Clearly, if the SAR could be maintained at its optimum value continuously, the result would be a minimum fuel flight. This is an important benchmark against which the energy efficiency of operations can be judged. However, as will be shown, holding SAR at its optimum value means that both the lift coefficient and, to a lesser extent, the flight Mach number must be continuously adjusted as the aircraft weight reduces due to fuel use. In operations, this usually means that the aircraft must climb continuously, following the so-called "cruise-climb" trajectory. In this situation, it is often assumed that any changes in the flight Reynolds number are negligibly small, in which case the SAR is inversely proportional to the instantaneous mass, and integration over distance travelled gives the well-known range equation that is often attributed to aviation pioneer Louis Breguet.[1] However, in reality, as the aircraft climbs, the Reynolds number changes, as do the operational optimum values of Mach number, lift coefficient and, most importantly, the SAR. Consequently, the SAR is no longer inversely proportional to the mass, and the simple classical Breguet range equation must always be subject to some degree of error.

The rapidly improving understanding of the environmental impact of aviation and the tremendous cost of reducing carbon dioxide emissions has placed increasing demands upon the accuracy of estimation methods for fuel requirements. In this paper, the effects of the Reynolds number upon the operational

[1] There appears to be no clear evidence that this equation is due to aviation pioneer Louis Breguet.

https://doi.org/10.1017/aer.2026.10264 Published online by Cambridge University Press

optimum conditions are examined and quantified; simple methods for accurate estimates are provided, and an improved version of the classic range equation is presented.

2.0 Background

As described in Reference [4], starting with the engine overall efficiency, η_o, defined as

$$\eta_o = \frac{nF_n V_\infty}{\dot{m}_f LCV} \tag{1}$$

where n is the number of engines, F_n is the net, installed thrust per engine, V_∞ is the true airspeed, $\dot{m}_f$ is the fuel mass flow per unit time and LCV is the lower calorific value of the fuel, the instantaneous SAR is given by

$$SAR = \frac{dS}{dm_f} = \frac{V_\infty}{\dot{m}_f} = \left(\frac{D}{nF_n}\right)\left(\frac{(\eta_o L/D)\, LCV}{L}\right) \tag{2}$$

Here, S is the distance travelled through the air, L is the total lift, and D is the total drag.

In the steady-state cruise, lift is equal to weight and thrust is equal to drag.[2] Hence,

$$\frac{dS}{dm_f} = -\frac{dS}{dm} = \left(\frac{(\eta_o L/D)\, LCV}{mg}\right) \tag{3}$$

where m is the instantaneous total mass of the aircraft and g is the acceleration due to gravity. Therefore, in cruise, the SAR is governed by the instantaneous mass, m, and the single aero-thermodynamic parameter $(\eta_o L/D)$. For this reason, $(\eta_o L/D)$ is sometimes referred to as the 'range parameter' (see, for example, Torenbeeck [5]).

In normal operations, aircraft do not cruise at specific values of geometric altitude. Rather, to maintain safe separation in the vertical direction, they follow isobars, i.e. the altitude is constantly modulated so that the local static pressure, p_∞, is held constant. By international agreement, values of local static pressure are converted into non-dimensional FLs. These are the geopotential altitudes, measured in feet, that the aircraft would have if it were operating in the ISA [1] made non-dimensional by dividing by 100 feet. For example, if the local static pressure measured by the aircraft air data system is 238.42 hPa, the geopotential altitude in the ISA would be 35,000 feet and, hence, the aircraft would be flying at FL 350.

3.0 Conditions for optimum $(\eta_o L/D)$ and the design optimum

In Poll and Schumann [2], it was shown that, for a given aircraft operating at fixed Mach number in steady, straight and level flight, there is a lift coefficient, $(C_L)_B$, at which $(\eta_o L/D)$ has a local maximum, or best, value. Furthermore, there is a particular Mach number and lift coefficient combination at which $(\eta_o L/D)$ reaches an absolute maximum, or optimum, level. The conditions for optimum $(\eta_o L/D)$ are determined by a balance between the gradients of η_o and L/D with respect to both Mach number, M_∞, and either FL or local static pressure, p_∞, i.e. when

$$d\,(\eta_o L/D) = \frac{\partial\,(\eta_o L/D)}{\partial M_\infty} dM_\infty + \frac{\partial\,(\eta_o L/D)}{\partial p_\infty} dp_\infty = 0 \tag{4}$$

In a steady, straight and level cruise, using the usual definitions for the aircraft lift, drag and thrust coefficients,

$$C_L = \frac{L}{q_\infty S_{ref}} \approx \frac{mg}{q_\infty S_{ref}} \text{ and } C_D = \frac{D}{q_\infty S_{ref}} \approx C_T = \frac{nF_n}{q_\infty S_{ref}} \tag{5}$$

[2] In general, the engine thrust line will not be parallel to the flight direction and thrust will have components in both the lift and drag directions. However, for a civil transport aircraft the differences are very small and may be neglected without significant loss of accuracy.

https://doi.org/10.1017/aer.2026.10264 Published online by Cambridge University Press

where S_{ref} is the wing reference area and, if γ is the ratio of specific heats for air,

$$q_\infty = \frac{\gamma}{2} p_\infty M_\infty^2 \tag{6}$$

Combining Equations (5) and (6) and taking m to be constant, partial differentiation of the lift coefficient with respect to M_∞ and p_∞ gives

$$\frac{M_\infty}{C_L}\left(\frac{\partial C_L}{\partial M_\infty}\right)^p = -2 \text{ and } \frac{p_\infty}{C_L}\left(\frac{\partial C_L}{\partial p_\infty}\right)^M = -1 \tag{7}$$

Here, the superscripts p and M indicate derivatives at constant static pressure and constant Mach number, respectively. Therefore, Equation (4) is satisfied when

$$\frac{M_\infty}{\eta_o}\frac{\partial \eta_o}{\partial M_\infty} - \frac{M_\infty}{Cd}\frac{\partial C_D}{\partial M_\infty} - 2 = 0 \tag{8}$$

and

$$\frac{C_L}{C_D}\frac{\partial C_D}{\partial C_L}\left(1 - \frac{C_T}{\eta_o}\frac{\partial \eta_o}{\partial C_T}\right) - 1 = 0 \tag{9}$$

As described in Poll and Schumann [2], the drag coefficient, C_D, is a function of aircraft geometry, C_L, M_∞ and the Reynolds number, R^{ac}, where

$$R^{ac} = \frac{l\rho_\infty V_\infty}{\mu_\infty} = S_{ref}^{1/2}\left(\frac{\gamma p_\infty M_\infty}{a_\infty \mu_\infty}\right) \tag{10}$$

Here, ρ_∞ is the air density, a_∞ is the local speed of sound and μ_∞ is the air dynamic viscosity. It follows that

$$C_D = C_D\,(C_L, M_\infty \text{and } R^{ac}) \tag{11}$$

Referring to the example shown in Figure 1, when the atmosphere is specified and the mass and flight Mach number are fixed, the aircraft lift-to-drag ratio has a local maximum at a particular value of the drag coefficient (and, hence, a particular lift coefficient). The maximum L/D reduces as the Mach number increases. In this case, C_D is varied by changing the FL.

Similarly, as described in Poll and Schumann [3] and as shown in Figure 2, at fixed M_∞, engine overall efficiency, η_o, has a local maximum value at a particular value of the thrust coefficient, C_T. This maximum value increases as the Mach number increases and, provided that M_∞ is greater than 0.2,[3] it may be represented by a power law, i.e. when

$$\frac{C_T}{\eta_o}\frac{\partial \eta_o}{\partial C_T} = 0 \tag{12}$$

$$(\eta_o)_B \approx \eta_1\,(M_\infty)^{\eta_2} \tag{13}$$

where the coefficients η_1 and η_2 are constant and depend upon the engine type. It follows that

$$\left(\frac{M_\infty}{\eta_o}\frac{\partial \eta_o}{\partial M_\infty}\right)_B = \eta_2 \tag{14}$$

In order to have the absolute maximum value of ($\eta_o L/D$), the airframe and engine must be perfectly matched, i.e. both η_o and L/D must have local maxima at the same values of M_∞ and C_D (=C_T). The locus of $(\eta_o)_{max}$ is shown in Figure 2 together with the locus of $(L/D)_{max}$ cross-plotted from Figure 1. The absolute maximum value of ($\eta_o L/D$) occurs at the loci intersection point. In this example, this corresponds to an M_∞ of 0.8, C_D of 0.033, C_L of 0.528 and an ($\eta_o L/D$) of 5.03.

[3] Equation (11) gives the correct value of $(\eta_o)_B$ when M_∞ is zero. However, with the exception of the special case when η_2 is unity, the gradient of $(\eta_o)_B$ with respect to M_∞ when M_∞ is zero is infinite and this cannot be correct. To avoid this problem, Equation (11) should only be used when M_∞ is greater than about 0.2.

https://doi.org/10.1017/aer.2026.10264 Published online by Cambridge University Press

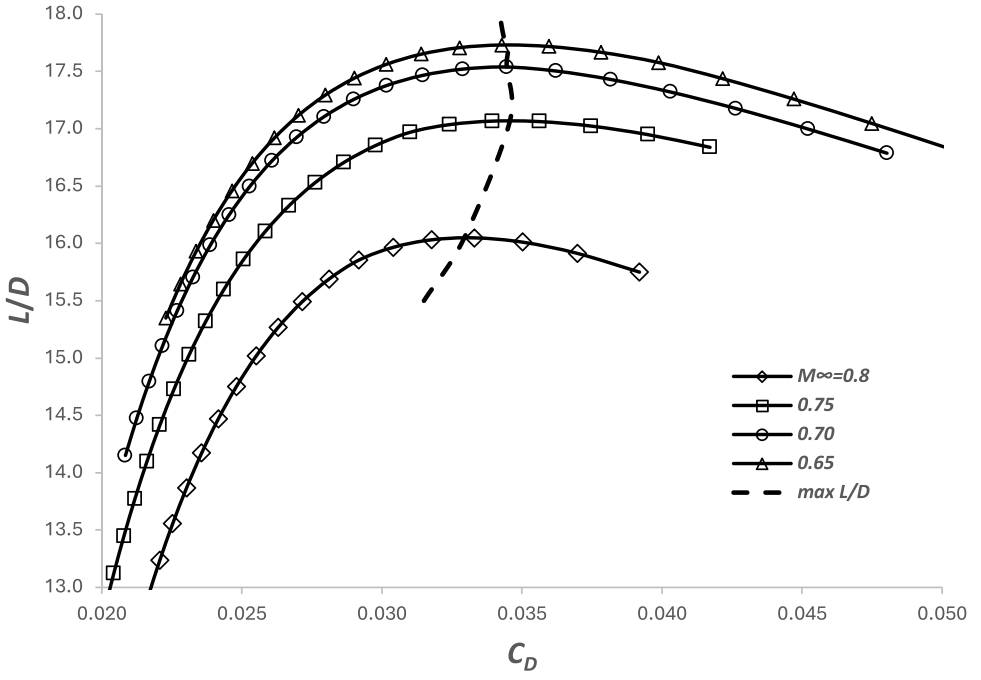


Figure 1. *An example of the variation of aircraft lift-to-drag ratio with drag coefficient and Mach number in the ISA when the mass is fixed. Figure taken from Poll and Schumann [2].*

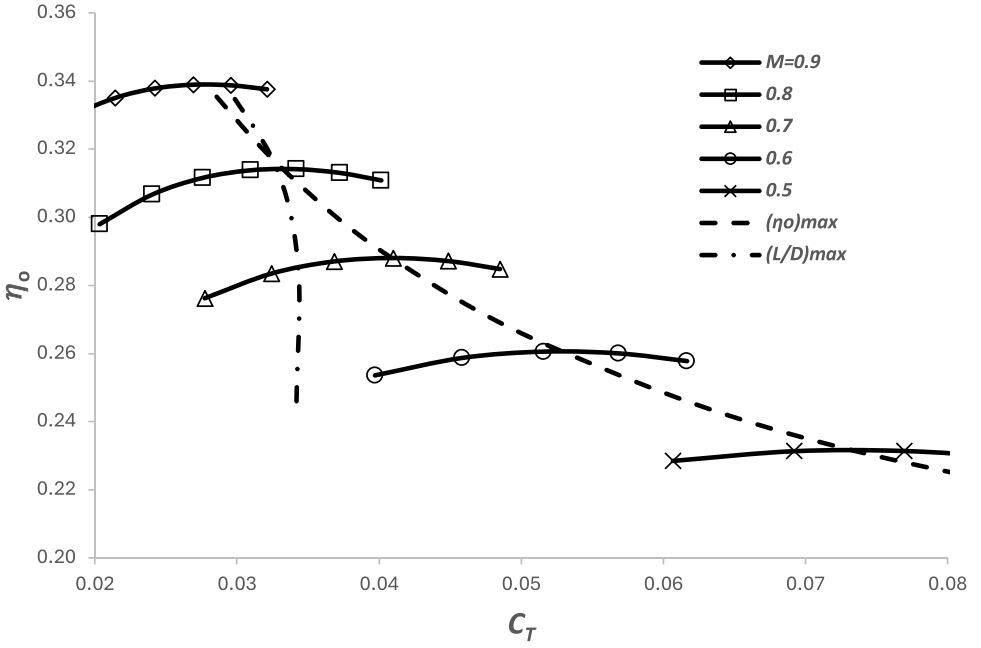


Figure 2. *The variation of overall efficiency with drag (=thrust) coefficient and Mach number for a civil aircraft turbofan engine with a nominal bypass ratio of 8. Figure taken from Poll and Schumann [3].*

https://doi.org/10.1017/aer.2026.10264 Published online by Cambridge University Press

From the definition of the Reynolds number given in Equation (10) and noting that a_∞ and μ_∞ only depend upon temperature, when the variation of temperature with pressure in the atmosphere is specified,

$$a_\infty \mu_\infty = function(p_\infty) \tag{15}$$

Therefore,

$$p_\infty = function\left(M_\infty, R^{ac} \text{ and } S_{ref}\right) \tag{16}$$

From the definition of lift coefficient,

$$C_L = \frac{2mg}{\gamma p_\infty M_\infty^2 S_{ref}} = function\left(m, S_{ref}, M_\infty \text{ and } R^{ac}\right) \tag{17}$$

and, from Equation (11),

$$C_D = C_D\left(C_L, M_\infty \; and \; R^{ac}\right) = function\left(m, S_{ref}, M_\infty \text{ and } R^{ac}\right) \tag{18}$$

Hence, for a given aircraft and engine combination, operating in a specified, single-valued,[4] atmosphere, e.g. the ISA, at specified values of M_∞, C_L and C_D, there is only one possible combination of mass, m, and R^{ac}, i.e. one m and FL pair. Since this operating point is effectively determined in the design process, it is appropriate to call it the "design" optimum condition.

At the design optimum, Equations (12) and (14) apply, and Equations (8) and (9) become

$$\left(\frac{M_\infty}{C_D}\frac{\partial C_D}{\partial M_\infty}\right)_{DO} = \eta_2 - 2 \tag{19}$$

and

$$\left(\frac{C_L}{C_D}\frac{\partial C_D}{\partial C_L}\right)_{DO} = 1 \tag{20}$$

These are completely general relations that define the design optimum value of $(\eta_o L/D)$ for the design mass, m_{des}, in the specified design atmosphere and the conditions at which it occurs.

Whilst the actual design conditions are known only to the manufacturer, in Reference [2], it was shown that, in general, the design optimum conditions can be expressed in terms of a mean skin-friction coefficient, C_F, defined as

$$C_F^{ac} \approx \frac{a}{(R^{ac})^b} = \frac{0.0269}{(R^{ac})^{0.14}} \tag{21}$$

and a parameter, Γ, that captures the atmospheric effects (see Appendix A), i.e.

$$\Gamma \approx 38.97(1 - \overline{\Delta T})L_h \tag{22}$$

Here, L_h is the vertical temperature lapse with respect to geopotential height, having units of K/m and the temperature term

$$\overline{\Delta T} = \frac{\Delta T}{(T_{TP})_{ISA}} \tag{23}$$

[4] A 'single-valued' atmosphere is one in which there is just one value of temperature for each value of pressure.

https://doi.org/10.1017/aer.2026.10264 Published online by Cambridge University Press

where ΔT is the local static temperature difference between the atmosphere and the ISA. This being the case, at the design condition,

$$(\eta_o L/D)_{DO} \approx (1 + 0.08b(1 + \Gamma_{DO}))\psi_1 \left(\frac{1}{C_F^{ac}}\right)_{DO}^{\left(\frac{1+\tau}{2}\right)} \tag{24}$$

$$(C_L)_{DO} \approx (1 - 0.60b(1 + \Gamma_{DO}))\psi_2 \left(C_F^{ac}\right)_{DO}^{\left(\frac{1-\tau}{2}\right)} \tag{25}$$

$$(L/D)_{DO} \approx (1 + 0.08b(1 + \Gamma_{DO}))\psi_3 \left(\frac{1}{C_F^{ac}}\right)_{DO}^{\left(\frac{1+\tau}{2}\right)} \tag{26}$$

and

$$M_{DO} \approx \psi_4 \tag{27}$$

The parameters ψ_{1-4} and τ are aircraft-dependent constants originally introduced in Poll and Schumann [7].

When aircraft performance estimates are required for the various phases of flight over a wide range of aircraft mass, Mach number and FL, the Poll-Schumann (P-S) method calculates the difference between the specified conditions and the design optimum values. Therefore, the design optimum conditions are inputs to the P-S method and their accuracy controls the overall accuracy of the output. Consequently, a great deal of effort has been focused upon producing the best possible estimates for the design optimum conditions of the various aircraft.

Since neither the value of an aircraft's design mass, m_{des}, nor the details of the design atmosphere are in the public domain, it is necessary to make some assumptions. In the P-S method, m_{des} is taken to be 80% of a reference maximum take-off mass,[5] $(\text{MTOM})_{ref}$, which is broadly typical of an average, mid-flight mass. In addition, the design atmosphere is taken to be the ISA, i.e. $(\Delta T)_{DO}$ is equal to zero at the design optimum condition. As shown in Appendix A, when the design optimum conditions occur in the ISA troposphere, $(\Gamma)_{DO}$ is equal to -0.255, whilst in the ISA stratosphere, $(\Gamma)_{DO}$ is zero. Based upon this definition, an initial set of best estimates for the parameters necessary to obtain the design optimum conditions using Equations (24) to (27) for 67 aircraft was given in Table 2 of Poll and Schumann [4]. This data set has now been updated and extended, with the corresponding coefficients for 71 aircraft being given in Table 1. The values presented in Table 1 supersede all previous versions.

In its current form, the P-S method is not valid for turboprop engines. This is because, as set out in detail in Poll and Schumann[3], the P-S engine model relies upon very specific dimensional analysis arguments that are only valid for turbofan engines. Consequently, in the case of the turboprop, the variation of η_o with C_T and M_∞ does not have the form shown in Figure 2, and the simple relation given in Equation (13) is not applicable. The basic physics of the turboprop is much more complicated, and further work needs to be done if the method is to be extended to cover this type of engine. However, whilst turboprop-powered aircraft currently account for 20% to 25% of the global fleet, since they operate exclusively on short-haul routes, they deliver only about 3% of the annual available seat kilometres flown globally. Consequently, in terms of the global annual fuel usage, turboprops are responsible for less than 3% of the total, whilst the turbofan aircraft in the current P-S data bank account for over 90%.

4.0 Operational optimum conditions

When either the aircraft mass is not equal to the design mass, or the variation of atmospheric temperature with pressure differs from the ISA, or both, as the FL is varied at a given flight Mach number, the

[5] Many aircraft are produced with a range of certified values of *MTOM* and $(MTOM)_{ref}$ is a typical mid-range value. Whilst m_{des} is an important, fixed characteristic of the aircraft, $(MTOM)_{ref}$ is only used to produce convenient, non-dimensional coefficients. Consequently, it cancels out when the method is applied and its value does not affect the results.

https://doi.org/10.1017/aer.2026.10264 Published online by Cambridge University Press

https://doi.org/10.1017/aer.2026.10264 Published online by Cambridge University Press

Table 1. *Revised estimates of the P-S characteristic parameters for a range of aircraft*

ICAO	$(MTOM)_{ref}$	m_{des}	Γ_{DO}	$(C_F)_{DO}$	τ	η_2	ψ_1	ψ_2	ψ_3	ψ_4	ψ_5	ψ_6
A30B	165000	132000	−0.255	2.063E−03	0.150	0.545	0.122	8.104	0.444	0.753	9.17E+07	0.693
A306	170500	136400	−0.255	2.044E−03	0.134	0.538	0.157	8.081	0.501	0.753	9.17E+07	0.716
A310	138600	110880	0.000	2.100E−03	0.163	0.536	0.155	8.038	0.464	0.772	8.63E+07	0.657
A313	150000	120000	−0.255	2.081E−03	0.159	0.537	0.155	8.066	0.475	0.772	8.63E+07	0.711
A318	68000	54400	0.000	2.223E−03	0.163	0.532	0.151	7.931	0.516	0.753	6.29E+07	0.607
A319	73500	58800	0.000	2.202E−03	0.166	0.522	0.142	7.962	0.503	0.753	6.29E+07	0.656
A320	73500	58800	0.000	2.214E−03	0.179	0.522	0.142	7.924	0.459	0.753	6.29E+07	0.656
A321	89000	71200	−0.255	2.167E−03	0.180	0.528	0.132	7.989	0.449	0.753	6.29E+07	0.794
A332	233000	186400	0.000	2.013E−03	0.149	0.535	0.192	8.088	0.590	0.786	1.13E+08	0.645
A333	233000	186400	0.000	2.016E−03	0.153	0.534	0.197	8.087	0.572	0.786	1.13E+08	0.645
A338	242000	193600	0.000	2.008E−03	0.151	0.445	0.231	8.086	0.642	0.786	1.15E+08	0.648
A339	242000	193600	0.000	2.013E−03	0.156	0.445	0.222	8.081	0.617	0.786	1.15E+08	0.648
A342	257000	205600	−0.255	1.999E−03	0.156	0.498	0.183	8.110	0.562	0.786	1.13E+08	0.711
A343	257000	205600	−0.255	2.003E−03	0.161	0.498	0.178	8.103	0.537	0.786	1.13E+08	0.711
A345	372000	297600	−0.255	1.923E−03	0.135	0.479	0.193	8.159	0.595	0.796	1.26E+08	0.831
A346	368000	294400	−0.255	1.930E−03	0.141	0.479	0.191	8.169	0.568	0.796	1.26E+08	0.822
A359	275000	220000	0.000	1.988E−03	0.132	0.445	0.238	8.013	0.641	0.820	1.31E+08	0.569
A35K	316000	252484	0.000	1.959E−03	0.136	0.467	0.234	8.073	0.641	0.820	1.34E+08	0.625
A388	569000	455200	−0.255	1.859E−03	0.100	0.470	0.234	8.055	0.644	0.820	1.80E+08	0.620
BCS1	60781	48625	0.000	2.256E−03	0.172	0.393	0.172	7.846	0.528	0.754	6.10E+07	0.576
BCS3	67586	54069	0.000	2.227E−03	0.177	0.393	0.165	7.876	0.503	0.754	6.10E+07	0.641
A19N	69750	55800	0.000	2.235E−03	0.186	0.385	0.170	7.867	0.522	0.753	6.29E+07	0.623
A20N	79000	63200	0.000	2.196E−03	0.185	0.385	0.170	7.926	0.515	0.753	6.29E+07	0.705
A21N	93500	74800	−0.255	2.164E−03	0.196	0.385	0.166	7.920	0.481	0.753	6.29E+07	0.835

https://doi.org/10.1017/aer.2026.10264 Published online by Cambridge University Press

Table 1. *Continued*

ICAO	$(MTOM)_{ref}$	m_{des}	Γ_{DO}	$(C_F)_{DO}$	τ	η_2	ψ_1	ψ_2	ψ_3	ψ_4	ψ_5	ψ_6
B712	54884	43907	−0.255	2.241E−03	0.173	0.545	0.126	7.882	0.437	0.700	5.09E+07	0.748
B722	83820	67056	0.000	2.168E−03	0.133	0.627	0.113	7.773	0.465	0.770	7.31E+07	0.554
B732	52390	41650	0.000	2.247E−03	0.158	0.627	0.097	7.910	0.449	0.700	5.26E+07	0.669
B733	61236	48989	0.000	2.225E−03	0.171	0.534	0.113	7.940	0.416	0.729	5.56E+07	0.700
B734	68039	54431	−0.255	2.199E−03	0.164	0.534	0.116	7.984	0.433	0.729	5.57E+07	0.774
B735	60555	48444	0.000	2.216E−03	0.154	0.534	0.118	7.957	0.462	0.729	5.60E+07	0.681
B736	65544	52435	0.000	2.240E−03	0.163	0.527	0.150	7.910	0.518	0.758	6.39E+07	0.567
B737	70080	56064	0.000	2.221E−03	0.165	0.531	0.141	7.937	0.507	0.758	6.39E+07	0.607
B738	79016	63213	0.000	2.191E−03	0.173	0.533	0.136	7.973	0.473	0.758	6.39E+07	0.684
B739	85139	68111	−0.255	2.171E−03	0.168	0.533	0.138	8.007	0.490	0.758	6.39E+07	0.737
B37M	80285	64228	0.000	2.181E−03	0.168	0.458	0.174	7.992	0.517	0.763	6.36E+07	0.700
B38M	82644	66115	0.000	2.176E−03	0.173	0.458	0.168	7.991	0.498	0.763	6.36E+07	0.720
B39M	88314	70651	−0.255	2.167E−03	0.176	0.458	0.168	7.992	0.487	0.763	6.36E+07	0.770
B3XM	89765	71812	−0.255	2.165E−03	0.178	0.458	0.165	7.991	0.479	0.763	6.36E+07	0.783
B742	371900	297520	−0.255	1.914E−03	0.114	0.541	0.162	7.813	0.536	0.810	1.38E+08	0.687
B743	377800	302240	−0.255	1.908E−03	0.113	0.542	0.163	7.762	0.543	0.810	1.38E+08	0.698
B744	396894	317515	−0.255	1.908E−03	0.118	0.537	0.180	7.838	0.567	0.810	1.43E+08	0.685
B748	442253	353802	−0.255	1.892E−03	0.115	0.468	0.222	7.836	0.614	0.830	1.53E+08	0.669
B752	113400	90266	0.000	2.105E−03	0.125	0.542	0.166	8.043	0.548	0.772	8.02E+07	0.623
B753	122470	97976	−0.255	2.098E−03	0.132	0.542	0.159	8.097	0.516	0.772	8.02E+07	0.673
B762	179169	143335	−0.255	2.035E−03	0.129	0.538	0.177	7.928	0.552	0.772	9.81E+07	0.657
B763/300ER	158758	127006	0.000	2.048E−03	0.119	0.538	0.186	7.842	0.605	0.772	9.81E+07	0.582
B764	204116	163293	−0.255	2.026E−03	0.154	0.534	0.170	7.991	0.540	0.772	9.81E+07	0.748
B77L	347450	277960	−0.255	1.941E−03	0.140	0.486	0.214	8.121	0.613	0.811	1.27E+08	0.765
B772	286900	229520	−0.255	1.970E−03	0.127	0.490	0.201	8.024	0.608	0.811	1.27E+08	0.632

https://doi.org/10.1017/aer.2026.10264 Published online by Cambridge University Press

Table 1. *Continued*

ICAO	$(MTOM)_{ref}$	m_{des}	Γ_{DO}	$(C_F)_{DO}$	τ	η_2	ψ_1	ψ_2	ψ_3	ψ_4	ψ_5	ψ_6
B77W	351530	281224	−0.255	1.947E−03	0.152	0.489	0.195	8.136	0.557	0.811	1.27E+08	0.774
B773	299370	239496	−0.255	1.969E−03	0.137	0.507	0.197	8.079	0.557	0.811	1.27E+08	0.659
B788	227930	182344	0.000	2.024E−03	0.141	0.445	0.231	7.974	0.614	0.815	1.20E+08	0.563
B789	254011	200161	0.000	1.998E−03	0.141	0.445	0.229	8.019	0.608	0.815	1.20E+08	0.627
B78X	254011	203209	0.000	1.996E−03	0.143	0.448	0.218	8.028	0.597	0.815	1.20E+08	0.627
C919S	75100	60080	0.000	2.208E−03	0.173	0.411	0.368	7.945	0.515	0.753	6.42E+07	0.644
C919L	78900	63120	0.000	2.192E−03	0.172	0.411	0.368	7.971	0.517	0.753	6.42E+07	0.676
E75S	40370	32296	0.000	2.312E−03	0.153	0.533	0.117	7.892	0.487	0.733	5.04E+07	0.560
E75L	40370	32296	0.000	2.315E−03	0.155	0.533	0.115	7.892	0.479	0.733	5.04E+07	0.560
E135	20000	16000	0.000	2.459E−03	0.158	0.541	0.105	7.691	0.463	0.704	3.81E+07	0.487
E145	22000	17600	0.000	2.431E−03	0.163	0.543	0.108	7.732	0.445	0.704	3.81E+07	0.536
E170	37200	29760	0.000	2.344E−03	0.181	0.533	0.113	7.808	0.468	0.733	4.72E+07	0.589
E190	47790	38232	0.000	2.298E−03	0.178	0.534	0.130	7.886	0.485	0.758	5.31E+07	0.599
E195	48790	39032	0.000	2.297E−03	0.171	0.534	0.126	7.911	0.472	0.758	5.50E+07	0.569
E290	56400	45120	0.000	2.275E−03	0.168	0.386	0.185	7.936	0.561	0.758	6.00E+07	0.552
E295	61500	49200	0.000	2.267E−03	0.190	0.392	0.168	7.885	0.518	0.758	6.00E+07	0.602
MD82	67812	54250	0.000	2.223E−03	0.189	0.611	0.104	7.953	0.426	0.720	5.76E+07	0.721
MD83	72575	58568	−0.255	2.204E−03	0.186	0.611	0.103	7.992	0.432	0.720	5.76E+07	0.772
GLF5	41277	33022	0.000	2.334E−03	0.131	0.558	0.177	7.727	0.557	0.772	5.99E+07	0.406
CRJ9	38329	30663	0.000	2.306E−03	0.155	0.533	0.124	7.801	0.475	0.753	4.72E+07	0.607
DC93	48988	39190	0.000	2.276E−03	0.162	0.627	0.100	7.907	0.475	0.733	5.34E+07	0.606
RJ1H	44225	35380	−0.255	2.283E−03	0.187	0.534	0.087	8.043	0.399	0.650	4.32E+07	0.838

Table 2. *Coefficients A to H when ι_{oo} is equal to 0.75405*

ICAO	$A_{0.745}$	$B_{0.745}$	$C_{0.745}$	$E_{0.745}$	$F_{0.745}$	$G_{0\cdot745}$	$H_{0.745}$
A30B	1.095E+08	2.015E−03	4.612	0.5458	15.876	0.7538	1.267
A306	1.169E+08	1.997E−03	5.613	0.5169	17.165	0.7538	1.382
A310	9.735E+07	2.048E−03	5.990	0.5578	17.155	0.7751	1.169
A313	1.029E+08	2.032E−03	5.933	0.5610	17.383	0.7732	1.264
A318	6.628E+07	2.162E−03	5.640	0.5642	18.508	0.7562	1.066
A319	6.981E+07	2.146E−03	5.326	0.5690	18.278	0.7559	1.143
A320	6.787E+07	2.154E−03	5.500	0.5908	17.291	0.7560	1.101
A321	7.713E+07	2.116E−03	5.237	0.6037	17.138	0.7538	1.312
A332	1.308E+08	1.965E−03	7.273	0.5283	21.401	0.7895	1.211
A333	1.295E+08	1.968E−03	7.536	0.5355	20.994	0.7896	1.195
A338	1.331E+08	1.960E−03	8.046	0.5303	23.447	0.7890	1.213
A339	1.314E+08	1.964E−03	7.839	0.5396	22.879	0.7891	1.192
A342	1.370E+08	1.953E−03	6.809	0.5486	20.815	0.7877	1.293
A343	1.351E+08	1.956E−03	6.728	0.5589	20.261	0.7877	1.269
A345	1.809E+08	1.878E−03	6.770	0.5095	21.159	0.7973	1.626
A346	1.766E+08	1.884E−03	6.810	0.5206	20.532	0.7973	1.574
A359	1.450E+08	1.937E−03	7.855	0.4933	22.227	0.8237	1.143
A35K	1.576E+08	1.915E−03	8.041	0.4996	22.627	0.8233	1.242
A388	2.307E+08	1.815E−03	7.417	0.4441	20.907	0.8215	1.391
BCS1	6.088E+07	2.187E−03	5.706	0.5763	19.270	0.7574	0.990
BCS3	6.515E+07	2.167E−03	5.574	0.5854	18.805	0.7570	1.084
A19N	6.444E+07	2.170E−03	5.856	0.6010	19.995	0.7563	1.026
A20N	7.080E+07	2.142E−03	5.890	0.6001	19.870	0.7558	1.166
A21N	7.782E+07	2.113E−03	5.951	0.6267	19.242	0.7538	1.328
B712	6.064E+07	2.189E−03	4.862	0.5909	15.997	0.7011	1.261
B722	7.885E+07	2.110E−03	4.282	0.4992	15.414	0.7734	1.100
B732	6.019E+07	2.191E−03	3.871	0.5567	15.720	0.7029	1.191
B733	6.399E+07	2.172E−03	4.328	0.5781	15.227	0.7314	1.202
B734	6.935E+07	2.148E−03	4.359	0.5765	15.561	0.7297	1.339
B735	6.558E+07	2.165E−03	4.280	0.5502	16.101	0.7313	1.228
B736	6.403E+07	2.172E−03	5.551	0.5638	18.507	0.7613	0.996
B737	6.698E+07	2.158E−03	5.303	0.5676	18.295	0.7610	1.059
B738	7.195E+07	2.137E−03	5.265	0.5816	17.609	0.7606	1.167
B739	7.608E+07	2.120E−03	5.278	0.5824	17.994	0.7587	1.262
B37M	7.375E+07	2.129E−03	6.168	0.5730	18.998	0.7662	1.212
B38M	7.456E+07	2.126E−03	6.081	0.5813	18.601	0.7662	1.230
B39M	7.695E+07	2.117E−03	6.109	0.5963	18.345	0.7644	1.287
B3XM	7.756E+07	2.114E−03	6.058	0.5997	18.193	0.7644	1.301
B742	1.875E+08	1.869E−03	5.678	0.4560	17.902	0.8112	1.501
B743	1.914E+08	1.863E−03	5.720	0.4506	18.101	0.8112	1.543
B744	1.915E+08	1.863E−03	6.386	0.4626	19.214	0.8112	1.475
B748	2.035E+08	1.847E−03	7.290	0.4552	20.651	0.8312	1.466
B752	9.480E+07	2.056E−03	5.704	0.4965	17.977	0.7750	1.246
B753	9.716E+07	2.049E−03	5.597	0.5195	17.267	0.7732	1.291
B762	1.206E+08	1.988E−03	6.241	0.4977	18.653	0.7732	1.316
B763/300ER	1.150E+08	2.001E−03	6.360	0.4696	19.775	0.7749	1.230

https://doi.org/10.1017/aer.2026.10264 Published online by Cambridge University Press

Table 2. *Continued*

ICAO	$A_{0.745}$	$B_{0.745}$	$C_{0.745}$	$E_{0.745}$	$F_{0.745}$	$G_{0\cdot745}$	$H_{0.745}$
B764	1.249E+08	1.978E−03	6.492	0.5413	19.792	0.7732	1.378
B77L	1.695E+08	1.895E−03	7.629	0.5169	22.024	0.8118	1.476
B772	1.523E+08	1.924E−03	6.850	0.4928	20.747	0.8118	1.278
B77W	1.657E+08	1.901E−03	7.247	0.5390	20.747	0.8118	1.432
B773	1.528E+08	1.923E−03	7.054	0.5122	19.635	0.8118	1.283
B788	1.287E+08	1.970E−03	7.768	0.5085	21.660	0.8190	1.097
B789	1.395E+08	1.948E−03	7.760	0.5089	21.617	0.8188	1.222
B78X	1.387E+08	1.949E−03	7.465	0.5129	21.353	0.8186	1.214
C919S	6.920E+07	2.149E−03	12.566	0.5803	19.093	0.7560	1.099
C919L	7.197E+07	2.137E−03	12.564	0.5786	19.158	0.7558	1.159
E75S	5.085E+07	2.243E−03	4.149	0.5526	16.548	0.7366	1.004
E75L	5.058E+07	2.245E−03	4.109	0.5566	16.383	0.7366	0.997
E135	3.413E+07	2.372E−03	3.672	0.5623	15.497	0.7086	0.857
E145	3.628E+07	2.352E−03	3.852	0.5700	15.163	0.7082	0.931
E170	4.653E+07	2.271E−03	4.311	0.5989	17.183	0.7371	0.973
E190	5.327E+07	2.229E−03	4.979	0.5945	17.845	0.7613	0.998
E195	5.384E+07	2.225E−03	4.747	0.5840	17.007	0.7614	0.964
E290	5.790E+07	2.203E−03	6.002	0.5782	20.153	0.7620	0.945
E295	5.906E+07	2.197E−03	5.851	0.6139	19.984	0.7619	0.971
MD82	6.494E+07	2.168E−03	4.551	0.6128	16.505	0.7229	1.167
MD83	6.788E+07	2.154E−03	4.441	0.6191	16.617	0.7210	1.243
GLF5	5.055E+07	2.245E−03	5.999	0.5082	17.671	0.7769	0.789
CRJ9	5.071E+07	2.244E−03	4.426	0.5501	16.252	0.7560	1.093
DC93	5.615E+07	2.212E−03	4.038	0.5654	16.726	0.7368	1.062
RJ1H	5.311E+07	2.230E−03	3.427	0.6341	15.102	0.6510	1.318

maximum value of ($\eta_o L/D$) will not coincide with the local maxima for both η_o and L/D. In this case, maximum ($\eta_o L/D$) is still given in Equations (8) and (9), but general solutions are difficult to find.

However, as described in Poll and Schumann [4], the P-S method can be applied to any aircraft following a specified trajectory and the path dynamics yield the lift, drag and thrust at each Mach number and FL pair. Engine overall efficiency, η_o, is then estimated from M_∞ and C_T, whilst L/D is estimated from M_∞, C_L and C_d. Values of η_o, C_T, C_L and C_d are then used in Equation (2) to obtain the instantaneous SAR. Since the method uses relations based upon established aerodynamic theory, rather than relying upon high-order polynomial curve fitting of performance data, differentiation with respect to any parameter continues to yield reasonably accurate results. Therefore, in principle, the operational optimum conditions can be obtained analytically. However, the nature of the relations is such that an analytic solution would be extremely complicated. Therefore, the approach adopted here is to use the P-S method to obtain numerical solutions of Equation (4) in the m, M_∞ and FL parameter space and use these to calibrate simple, approximate relations for the optimum conditions.

Calculations have been carried out for two aircraft – one a single-aisle and the other a twin-aisle configuration. Possible instantaneous masses range from the minimum value, taken to be operational empty mass (OEM), plus reserve fuel, to the certified MTOM. In practise, neither of these quantities is completely determined, since the OEM depends upon the cabin configuration and each aircraft type is usually produced with a variety of certified values of MTOM. However, examination of the aircraft database shows that achievable values of m typically lie within the range

$$0.8\ (m_{des}) \leq m \leq 1.2\ (m_{des}) \tag{28}$$

https://doi.org/10.1017/aer.2026.10264 Published online by Cambridge University Press

In addition, the properties of the atmosphere on any given day may vary markedly from the ISA values. For this study, at a given value of p_∞, values of the temperature difference ΔT relative to the ISA have been taken to lie in the range

$$-20K \leq \Delta T \leq +30K \tag{29}$$

With the temperature vertical lapse rate, L_h, lying in the range

$$-0.02\ K/m \leq L_h \leq +0.02K/m \tag{30}$$

In Reference [2], it was suggested that estimates of the operational optimum conditions could be obtained by applying Equations (24) to (27) and assuming that the coefficients ψ_1, ψ_2 and ψ_4[6] were constant with their design optimum values, even though a weak Reynolds number dependence had been found. The numerical solutions show that this is a reasonable assumption for ψ_1, ψ_3 and ψ_4, which exhibit less than $\pm 1.5\%$ over the parameter range considered. However, in the case of ψ_2 the variation is found to be much larger, being in the region of $\pm 8\%$. Given the cost of fuel and the political sensitivity to carbon dioxide emissions, variations in fuel use of order 1% are deemed to be significant. Therefore, this simple approach is insufficiently accurate, and an improved estimation method is required.

In the new approach, the operational optimum $(\eta_o L/D)$ is obtained by combining $(\eta_o)_{OO}$ from Equation (13) and $(L/D)_{OO}$, i.e.

$$(\eta_o L/D)_{OO} = (\eta_o)_{OO}\ (L/D)_{OO} \approx \eta_1\ (M_{OO})^{\eta_2}\ (L/D)_{OO} \tag{31}$$

The other parameters depend only upon the airframe, and estimates are based upon the general form of Equations (25), (26) and (27), with the introduction of correction functions[7] f_2, f_3 and f_4, i.e.

$$(C_L)_{OO} = f_2\ (1 - 0.60b\ (1 + \Gamma_{OO}))\ \psi_2 \left(C_F^{ac}\right)_{OO}^{\left(\frac{1-\tau}{2}\right)} \tag{32}$$

$$(L/D)_{OO} = f_3\ (1 + 0.08b\ (1 + \Gamma_{OO}))\ \psi_3 \left(\frac{1}{C_F^{ac}}\right)_{OO}^{\left(\frac{1+\tau}{2}\right)} \tag{33}$$

and

$$M_{OO} = f_4.\psi_4 \tag{34}$$

where b is the constant coefficient in the skin friction relation given in Equation (21).

Experimentation with the numerical results reveals that, to a very good approximation, the f functions also have the general form

$$f \approx \frac{(1 + \beta.b\ (1 + \Gamma_{OO}))}{(1 + \beta.b\ (1 + \Gamma_{DO}))} \left(\frac{\left(C_F^{ac}\right)_{OO}}{\left(C_F^{ac}\right)_{DO}}\right)^{\delta} \tag{35}$$

where β and δ are constant coefficients, and f is equal to unity when conditions correspond to the design optimum values. Specifically, it is found that, for f_2, f_3 and f_4, the corresponding values for β and δ are

$$\beta_2 \approx 0.542,\ \delta_2 \approx -0.435 \tag{36}$$

$$\beta_3 \approx -0.062,\ \delta_3 \approx 0.0450 \tag{37}$$

and

$$\beta_4 \approx -0.0645,\ \delta_4 \approx -0.162 \tag{38}$$

Comparisons between these approximations and the numerical values for both the large and the small aircraft are shown in Figures 3, 4, 5 and 6. Agreement is better than $\pm 0.25\%$ in all cases.

[6] The parameters ψ_5 and ψ_7 only depend upon aircraft physical characteristics and so are invariant.

[7] There is no need for an f_1.

https://doi.org/10.1017/aer.2026.10264 Published online by Cambridge University Press

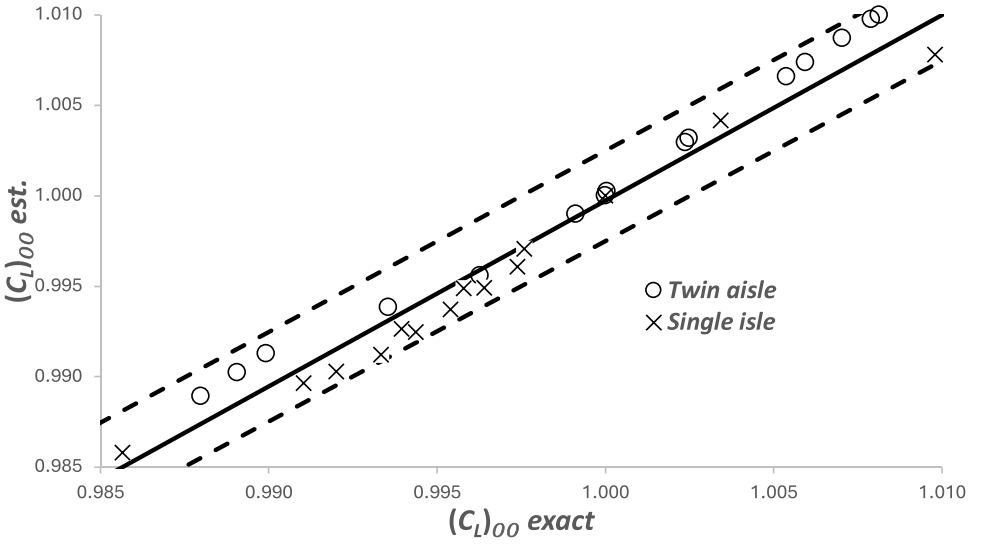


Figure 3. *Comparison between the estimated and the numerically exact values of the operational optimum lift coefficient for two aircraft types and a range of atmospheric conditions. The dashed lines show the ±0.25% deviation.*

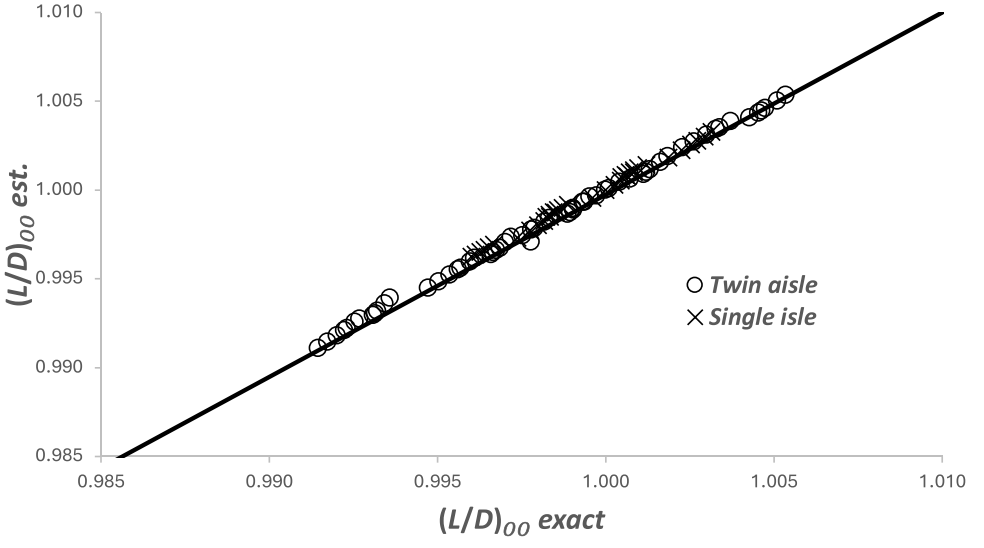


Figure 4. *Comparison between the estimated and the numerically exact values of the operational optimum lift-to-drag ratio for two aircraft types and a range of atmospheric conditions.*

4.1 Basic relations

In the analysis that follows, it is assumed that the engine can provide the necessary thrust at all conditions. However, gas turbine engines have well-defined operating limits that are functions of atmospheric temperature. Therefore, when performing estimates for a particular engine-airframe combination, it is important to check that the engine can deliver the required thrust. Estimates for the various engine limits are given in Poll and Schumann [3, 4].

https://doi.org/10.1017/aer.2026.10264 Published online by Cambridge University Press

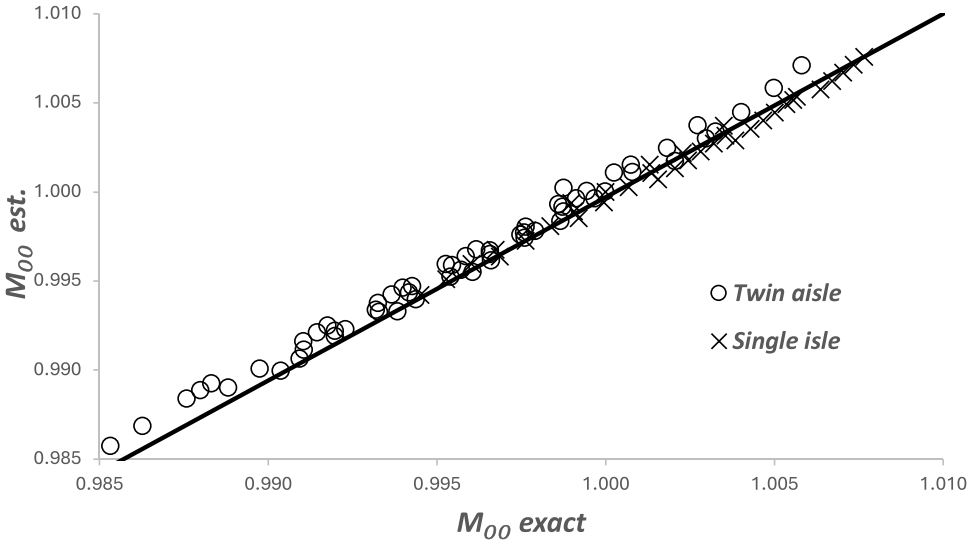


Figure 5. *Comparison between the estimated and the numerically exact values of the operational optimum Mach number for two aircraft types and a range of atmospheric conditions.*

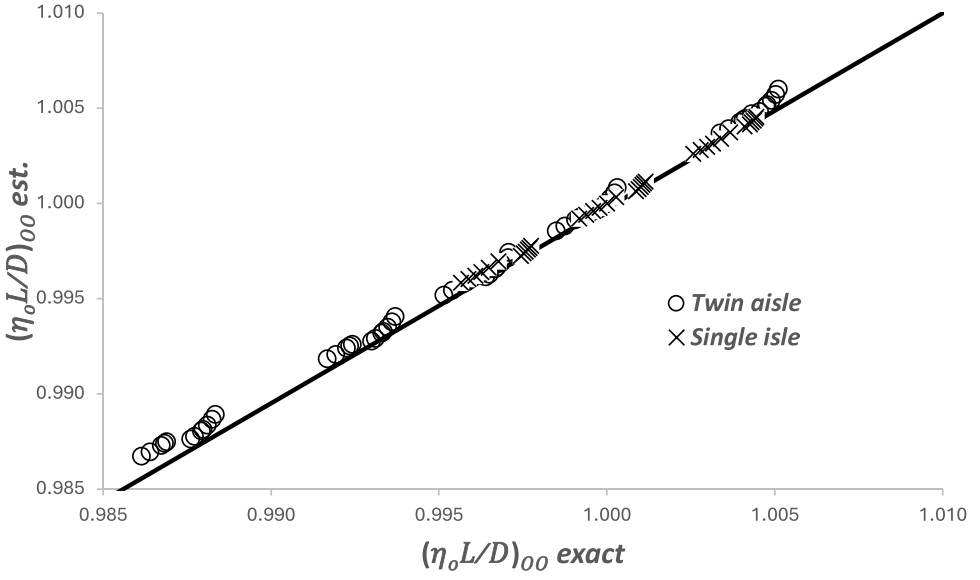


Figure 6. *Comparison between the estimated and the numerically exact values of the operational optimum range parameter for two aircraft types and a range of atmospheric conditions.*

Substituting the results from Equations (36) to (38) into Equations (32), (33) and (34), taking b to be 0.14 and ignoring terms that are less than 0.001 in comparison to unity, gives

$$(C_L)_{OO} \approx (1 - 0.021(\Gamma)_{OO})\, \xi_2 \left(C_F^{ac}\right)_{OO}^{\left(\frac{0.130-\tau}{2}\right)} \tag{39}$$

$$(L/D)_{OO} \approx (1 + 0.002(\Gamma)_{OO})\, \xi_3 \left(\frac{1}{C_F^{ac}}\right)_{OO}^{\left(\frac{0.910+\tau}{2}\right)} \tag{40}$$

https://doi.org/10.1017/aer.2026.10264 Published online by Cambridge University Press

$$M_{OO} \approx (1 - 0.009(\Gamma)_{OO})\, \xi_4 \left(\frac{1}{C_F^{ac}}\right)_{OO}^{0.162} \tag{41}$$

and, from Equation (31),

$$(\eta_o L/D)_{OO} \approx (1 - 0.002\,(4.0\eta_2 - 1)\,(\Gamma)_{OO})\, \xi_1 \left(\frac{1}{C_F^{ac}}\right)_{OO}^{\left(\frac{0.910(1+0.36\eta_2)+\tau}{2}\right)} \tag{42}$$

where

$$\xi_1 \approx \left(\eta_1 \xi_4^{\eta_2}\right) \xi_3 = \left(\frac{1.011}{1 - 0.009\,(1+\eta_2)\,(\Gamma)_{DO}}\right) \psi_1 \left(C_F^{ac}\right)_{DO}^{0.162(\eta_2 - 0.28)} \tag{43}$$

$$\xi_2 \approx \left(\frac{0.916}{1 + 0.0705(\Gamma)_{DO}}\right) \psi_2 \left(C_F^{ac}\right)_{DO}^{0.435} \tag{44}$$

$$\xi_3 \approx \left(\frac{1.011}{1 - 0.009(\Gamma)_{DO}}\right) \psi_3 \left(\frac{1}{C_F^{ac}}\right)_{DO}^{0.045} \tag{45}$$

and

$$\xi_4 \approx \left(\frac{1}{1 - 0.009(\Gamma)_{DO}}\right) \psi_4 \left(C_F^{ac}\right)_{DO}^{0.162} \tag{46}$$

The ξ parameters only depend upon the design conditions and, consequently, are characteristics of the aircraft and engine combination. Values are included in Table 1.

4.2 Reynolds number

As shown in Appendix A, the operational optimum value for the Reynolds number is given by

$$(R^{ac})_{OO} = S_{ref}^{1/2} \left(\frac{\gamma p_\infty M_\infty}{\mu_\infty a_\infty}\right)_{OO} \approx S_{ref}^{1/2} \left(\frac{\gamma p_{TP}}{\mu_{TP} a_{TP}}\right)_{ISA} \left(\frac{(p_\infty)_{OO}}{(p_{TP})_{ISA}}\right)^{\iota_{OO}} \left(\frac{M_{OO}}{1 + 1.34(\overline{\Delta T})}\right) \tag{47}$$

where ι_{OO} is equal to 0.74505 if p_∞ is greater than, or equal to, $(p_{TP})_{ISA}$; otherwise, ι_{OO} is equal to 1. The change in the value of ι_{OO} is necessary because the atmospheric temperature at a given pressure is measured relative to the ISA, and the ISA has a discontinuity in lapse rate when p_∞ is equal to $(p_{TP})_{ISA}$.

Using the definition of lift coefficient given in Equation (5), the Reynolds number may be expressed as

$$(R^{ac})_{OO} \approx \left(\frac{\psi_5}{1 + 1.34(\overline{\Delta T})_{OO}}\right) \left(\frac{\psi_4}{M_{OO}}\right)^{(2\iota_{OO}-1)} \left(\frac{\psi_6}{(C_L)_{OO}} \left(\frac{m}{MTOM_{ref}}\right)\right)^{\iota_{OO}} \tag{48}$$

where

$$\psi_5 = S_{ref}^{1/2} \left(\frac{\gamma p_{TP}}{\mu_{TP} a_{TP}}\right)_{ISA} \tag{49}$$

and

$$\psi_6 = \frac{MTOM_{ref}.g}{(\gamma/2)\,(p_{TP})_{ISA}\,\psi_4^2 S_{ref}} \tag{50}$$

The lift coefficient and Mach number are now eliminated by the use of Equations (41) and (43) leading to

$$(R^{ac})_{OO} \approx \left(\frac{\psi_5}{1 + 1.34(\overline{\Delta T})_{OO} - 0.020(\Gamma)_{OO}}\right) \left(\frac{\psi_4}{\xi_4}\right)^{0.4901} \left(\frac{\psi_6}{\xi_2} \left(\frac{m}{MTOM_{ref}}\right)\right)^{0.74505} \left(C_F^{ac}\right)_{OO}^{\left(\frac{\tau+0.083}{2.684}\right)} \tag{51}$$

when ι_{OO} is equal to 0.74505 and

$$(R^{ac})_{OO} \approx \left(\frac{\psi_5}{1 + 1.34(\overline{\Delta T})_{OO} - 0.030(\Gamma)_{OO}}\right) \left(\frac{\psi_4}{\xi_4}\right) \left(\frac{\psi_6}{\xi_2} \left(\frac{m}{MTOM_{ref}}\right)\right) \left(C_F^{ac}\right)_{OO}^{\left(\frac{\tau+0.194}{2}\right)} \tag{52}$$

https://doi.org/10.1017/aer.2026.10264 Published online by Cambridge University Press

when ι_{OO} is equal to unity.

From Equation (21),

$$\left(C_F^{ac}\right)_{OO} \approx \frac{0.0269}{\left(R^{ac}\right)_{OO}^{0.14}} \tag{53}$$

Hence, when ι_{OO} is 0.74505,

$$\left(R^{ac}\right)_{OO} \approx A_{0.745}\left(\left(\frac{1}{1+1.34(\overline{\Delta T})_{OO}-0.020(\Gamma)_{OO}}\right)\left(\frac{m}{MTOM_{ref}}\right)^{0.74505}\right)^{\left(\frac{0.996}{1+0.05\tau}\right)} \tag{54}$$

where

$$A_{0.74505} = (0.0269)^{0.371\left(\frac{\tau+0.083}{1+0.05\tau}\right)}\left(\psi_5\left(\frac{\psi_4}{\xi_4}\right)^{0.4901}\left(\frac{\psi_6}{\xi_2}\right)^{0.74505}\right)^{\left(\frac{0.996}{1+0.05\tau}\right)} \tag{55}$$

and when ι_{OO} is unity,

$$\left(R^{ac}\right)_{OO} \approx A_1\left(\left(\frac{1}{1+1.34(\overline{\Delta T})_{OO}-0.030(\Gamma)_{OO}}\right)\left(\frac{m}{MTOM_{ref}}\right)\right)^{\left(\frac{0.987}{1+0.07\tau}\right)} \tag{56}$$

where

$$A_1 \approx (0.0269)^{0.493\left(\frac{\tau+0.194}{1+0.07\tau}\right)}\left(\psi_5\left(\frac{\psi_4}{\xi_4}\right)\left(\frac{\psi_6}{\xi_2}\right)\right)^{\left(\frac{0.987}{1+0.07\tau}\right)} \tag{57}$$

The A values are included in Table 1.

As shown in Table 1, τ always lies in the range 0.1–0.2. Hence, without significant loss of accuracy, Equations (54) and (56) may be further simplified to

$$\left(R^{ac}\right)_{OO} \approx \left(\frac{A_{0.745}}{1+1.32(\overline{\Delta T})_{OO}-0.020(\Gamma)_{OO}}\right)\left(\frac{m}{MTOM_{ref}}\right)^{0.736} \tag{58}$$

and

$$\left(R^{ac}\right)_{OO} \approx \left(\frac{A_1}{1+1.31(\overline{\Delta T})_{OO}-0.030(\Gamma)_{OO}}\right)\left(\frac{m}{MTOM_{ref}}\right)^{0.976} \tag{59}$$

It follows that the value of aircraft mass, m_T, for which R^{ac} is the same for both values of ι_{oo} is

$$\left(\frac{m_T}{MTOM_{ref}}\right) \approx \left(1-0.06(\overline{\Delta T})_{OO}-0.039(\Gamma)_{OO}\right)\left(\frac{A_{0.745}}{A_1}\right)^{4.16} \tag{60}$$

This is the mass for which the optimum operational cruise FL is 360.89, and it is seen to be a weak function of the atmospheric parameters, with maximum likely deviations being of the order 1%.

Equation (60) is valid when ΔT and Γ are continuous functions of $p_{\infty,}$ and this is the most likely situation in real atmospheres. However, in theoretical studies, the operational atmosphere is often taken to be an ISA + ΔT where ΔT is constant. In this case, Γ is discontinuous when p_∞ is equal to $(p_{TP})_{ISA,}$ and it is easily shown that

$$\left(\frac{m_T}{MTOM_{ref}}\right) \approx 0.979\left(1-0.02(\overline{\Delta T})_{OO}\right)\left(\frac{A_{0.745}}{A_1}\right)^{4.16} \tag{61}$$

If m is greater than or equal to m_T, ι_{oo} is equal to 0.75405 and, if m is less than m_T, ι_{oo} is equal to unity. Therefore, depending upon the value of ι_{oo}, either Equation (58) or Equation (59) gives the Reynolds number at the optimum condition in terms of aircraft mass, m, the characteristics of the atmosphere, ΔT and Γ and fixed characteristics of the aircraft, ξ_2, ξ_4, $\psi_{4,}$ ψ_5, ψ_6 and τ.

https://doi.org/10.1017/aer.2026.10264 Published online by Cambridge University Press

4.3 Skin friction coefficient

With the operational optimum Reynolds number determined, the mean skin-friction coefficient follows from Equations (53), (58) and (59), i.e.

$$\left(C_F^{ac}\right)_{OO} \approx B_{0.745}\left(1 + 0.19(\overline{\Delta T})_{OO} - 0.003(\Gamma)_{OO}\right)\left(\frac{MTOM_{ref}}{m}\right)^{0.103} \tag{62}$$

and

$$\left(C_F^{ac}\right)_{OO} \approx B_1\left(1 + 0.18(\overline{\Delta T})_{OO} - 0.004(\Gamma)_{OO}\right)\left(\frac{MTOM_{ref}}{m}\right)^{0.137} \tag{63}$$

where B is

$$B = \frac{0.0269}{A^{0.14}} \tag{64}$$

4.4 Range parameter ($\eta_o L/D$)

The operational optimum value of $(\eta_o L/D)$ is obtained from Equations (42), (62) and (63). Again, neglecting terms that are less than 0.001 in comparison to unity, this becomes

$$(\eta_o L/D)_{OO} \approx C_{0.745}(1 - 0.11(\overline{\Delta T})_{OO})\left(\frac{m}{MTOM_{ref}}\right)^{\left(\frac{0.910(1+0.36\eta_2)+\tau}{19.41}\right)} \tag{65}$$

and

$$(\eta_o L/D)_{OO} \approx C_1(1 - 0.11(\overline{\Delta T})_{OO})\left(\frac{m}{MTOM_{ref}}\right)^{\left(\frac{0.910(1+0.36\eta_2)+\tau}{14.63}\right)} \tag{66}$$

where

$$C = \xi_1\left(\frac{1}{B}\right)^{\left(\frac{0.910(1+0.36\eta_2)+\tau}{2}\right)} \tag{67}$$

4.5 Lift coefficient

The operational optimum lift coefficient comes from Equations (39), (62) and (63), i.e.

$$(C_L)_{OO} \approx E_{0.745}\left(1 - 0.021(\Gamma)_{OO}\right)\left(\frac{m}{MTOM_{ref}}\right)^{\left(\frac{\tau-0.130}{19.41}\right)} \tag{68}$$

and

$$(C_L)_{OO} \approx E_1\left(1 - 0.021(\Gamma)_{OO}\right)\left(\frac{m}{MTOM_{ref}}\right)^{\left(\frac{\tau-0.130}{14.63}\right)} \tag{69}$$

where

$$E = \xi_2\,(B)^{\left(\frac{0.130-\tau}{2}\right)} \tag{70}$$

4.6 Lift-to-drag ratio

The operational optimum lift-to-drag ratio comes from Equations (40), (62) and (63), i.e.

$$(L/D)_{OO} \approx F_{0.745}\left(1 - 0.10(\overline{\Delta T})_{OO} + 0.004(\Gamma)_{OO}\right)\left(\frac{m}{MTOM_{ref}}\right)^{\left(\frac{0.910+\tau}{19.41}\right)} \tag{71}$$

and

$$(L/D)_{OO} \approx F_1\left(1 - 0.10(\overline{\Delta T})_{OO} + 0.004(\Gamma)_{OO}\right)\left(\frac{m}{MTOM_{ref}}\right)^{\left(\frac{0.910+\tau}{14.63}\right)} \tag{72}$$

https://doi.org/10.1017/aer.2026.10264 Published online by Cambridge University Press

where

$$F = \xi_3 \left(\frac{1}{B}\right)^{\left(\frac{0.910+\tau}{2}\right)} \tag{73}$$

4.7 Mach number

The operational optimum Mach number comes from Equations (41), (62) and (63), i.e.

$$M_{OO} \approx G_{0.745}(1 - 0.03(\overline{\Delta T})_{OO} - 0.009(\Gamma)_{OO}) \left(\frac{m}{MTOM_{ref}}\right)^{0.017} \tag{74}$$

and

$$M_{OO} \approx G_1(1 - 0.03(\overline{\Delta T})_{OO} - 0.008(\Gamma)_{OO}) \left(\frac{m}{MTOM_{ref}}\right)^{0.022} \tag{75}$$

where

$$G = \xi_4 \left(\frac{1}{B}\right)^{0.162} \tag{76}$$

4.8 Flight level

From the definition of lift coefficient and using Equation (50)

$$(C_L)_{OO} = \frac{m.g}{\frac{\gamma}{2}(p_\infty)_{OO} M_{OO}^2 S_{ref}} = \psi_6 \left(\frac{(p_{TP})_{ISA}}{(p_\infty)_{OO}}\right) \left(\frac{\psi_4}{M_{OO}}\right)^2 \left(\frac{m}{(MTOM)_{ref}}\right) \tag{77}$$

Hence, the static pressure at the optimum operational altitude is

$$\frac{(p_\infty)_{OO}}{(p_{TP})_{ISA}} = \left(\frac{\psi_6}{(C_L)_{OO}}\right) \left(\frac{\psi_4}{M_{OO}}\right)^2 \left(\frac{m}{(MTOM)_{ref}}\right) \tag{78}$$

Once again, the evaluation of $(C_L)_{OO}$ and M_{OO} requires the specification of ι, and this is obtained by comparing m with m_T from Equation (60), or Equation (61). As already noted, if m is greater than or equal to m_T, ι_{oo} is equal to 0.75405 and, using Equations (68) and (74),

$$\frac{(p_\infty)_{OO}}{(p_{TP})_{ISA}} \approx H_{0.745} \left(1 + 0.06(\overline{\Delta T})_{OO} + 0.039(\Gamma)_{OO}\right) \left(\frac{m}{(MTOM)_{ref}}\right)^{\left(\frac{18.89-\tau}{19.41}\right)} \tag{79}$$

whilst, if m is less than m_T, ι_{oo} is equal to unity and, from Equations (69) and (75),

$$\frac{(p_\infty)_{OO}}{(p_{TP})_{ISA}} \approx H_1(1 + 0.06(\overline{\Delta T})_{OO} + 0.038(\Gamma)_{OO}) \left(\frac{m}{(MTOM)_{ref}}\right)^{\left(\frac{14.11-\tau}{14.63}\right)} \tag{80}$$

where

$$H = \left(\frac{\psi_6}{E}\right) \left(\frac{\psi_4}{G}\right)^2 \tag{81}$$

Using the relations given in Poll and Schumann [1], local static pressure is linked directly to the FL and, if $(p_\infty)_{OO}$ is greater than $(p_{TP})_{ISA}$,

$$FL_{OO} = 1454.42 \left(1 - 0.751865 \left(\frac{(p_\infty)_{OO}}{(p_{TP})_{ISA}}\right)^{0.190263}\right) \tag{82}$$

otherwise

$$FL_{OO} = 360.892 \left(1 - 0.576511 ln \left(\frac{(p_\infty)_{OO}}{(p_{TP})_{ISA}}\right)\right) \tag{83}$$

https://doi.org/10.1017/aer.2026.10264 Published online by Cambridge University Press

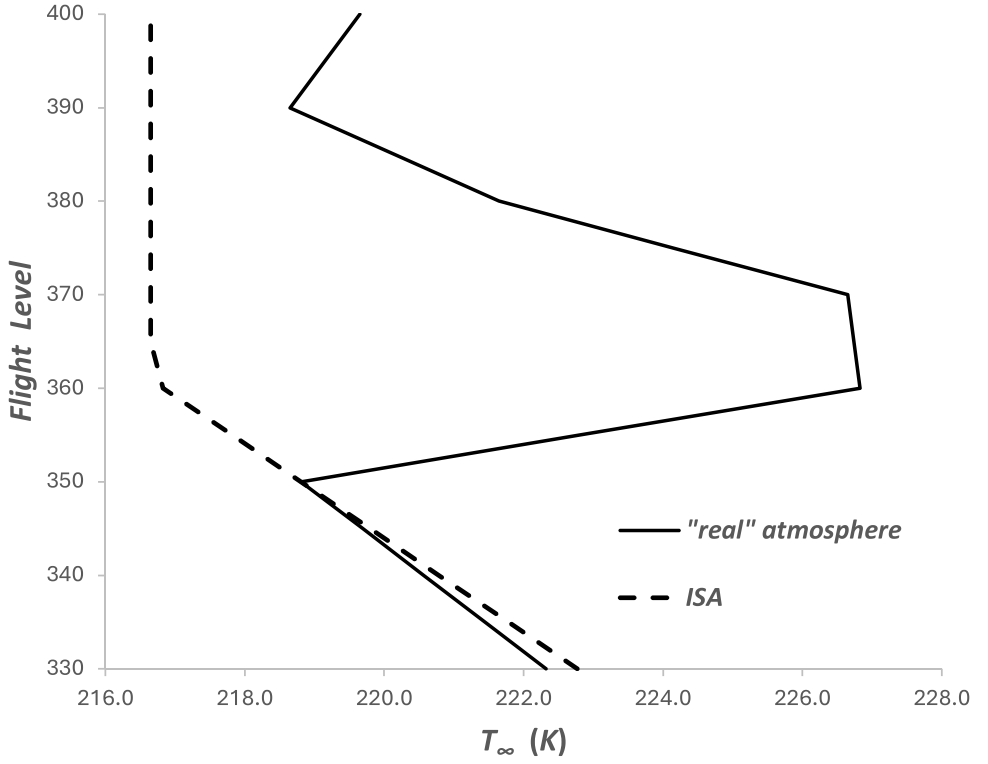


Figure 7. *An example of an observed variation of atmospheric temperature with FL compared with that in the ISA. Figure taken from Poll and Schumann [9].*

4.9 True airspeed

From the definition of Mach number, the true airspeed, V_{OO}, is given by

$$V_{OO} = M_{OO}\sqrt{(\gamma \Re T_{OO})} = M_{OO}\sqrt{(\gamma \Re (T_{TP})_{ISA})}\left(\left(\frac{T}{T_{TP}}\right)_{ISA} + \overline{\Delta T}\right)^{\frac{1}{2}}_{OO} \tag{84}$$

From Reference [1], if FL_{OO} is less than or equal to 360.892,

$$\left(\frac{T}{T_{TP}}\right)_{ISA} = 1.3300 - 0.0009144\,(FL_{oo}) \tag{85}$$

and, if FL_{OO} is greater than 360.892,

$$\left(\frac{T}{T_{TP}}\right)_{ISA} = 1.0 \tag{86}$$

Values of the coefficients A to G when ι_{oo} is equal to 0.75405 are given in Table 2 and values A to G when ι_{oo} is equal to 1 are given in Table 3.

5.0 Sample calculation

An example of an observed variation of atmospheric temperature with pressure obtained by a weather balloon, originally used in Poll and Schumann [9], is given in Figure 7 together with the variation in the ISA. Clearly, whilst the variation of temperature with pressure (FL) in the ISA is monotonically

https://doi.org/10.1017/aer.2026.10264 Published online by Cambridge University Press

Table 3. *Coefficients A to H when ι_{oo} is equal to1*

ICAO	$A_{1.0}$	$B_{1.0}$	$C_{1.0}$	$E_{1.0}$	$F_{1.0}$	$G_{1.0}$	$H_{1.0}$
A30B	1.161E+08	1.998E−03	4.635	0.5458	15.946	0.7549	1.263
A306	1.267E+08	1.974E−03	5.651	0.5169	17.266	0.7552	1.377
A310	1.012E+08	2.037E−03	6.010	0.5578	17.205	0.7758	1.167
A313	1.091E+08	2.016E−03	5.963	0.5610	17.459	0.7742	1.261
A318	6.734E+07	2.157E−03	5.648	0.5642	18.530	0.7564	1.065
A319	7.218E+07	2.136E−03	5.341	0.5690	18.324	0.7564	1.142
A320	6.952E+07	2.147E−03	5.512	0.5908	17.323	0.7564	1.100
A321	8.252E+07	2.096E−03	5.268	0.6038	17.227	0.7550	1.308
A332	1.372E+08	1.952E−03	7.303	0.5283	21.476	0.7904	1.209
A333	1.354E+08	1.956E−03	7.565	0.5355	21.064	0.7904	1.192
A338	1.397E+08	1.947E−03	8.078	0.5304	23.531	0.7899	1.210
A339	1.373E+08	1.952E−03	7.868	0.5397	22.954	0.7899	1.189
A342	1.460E+08	1.935E−03	6.846	0.5487	20.914	0.7888	1.289
A343	1.434E+08	1.940E−03	6.763	0.5590	20.351	0.7887	1.265
A345	2.042E+08	1.846E−03	6.840	0.5095	21.347	0.7995	1.617
A346	1.977E+08	1.855E−03	6.875	0.5207	20.703	0.7994	1.566
A359	1.499E+08	1.928E−03	7.877	0.4933	22.281	0.8243	1.141
A35K	1.664E+08	1.900E−03	8.078	0.4996	22.716	0.8243	1.239
A388	2.505E+08	1.794E−03	7.467	0.4440	21.029	0.8230	1.386
BCS1	6.072E+07	2.188E−03	5.705	0.5763	19.266	0.7574	0.990
BCS3	6.647E+07	2.161E−03	5.584	0.5854	18.833	0.7574	1.083
A19N	6.485E+07	2.168E−03	5.859	0.6010	20.005	0.7564	1.026
A20N	7.355E+07	2.130E−03	5.909	0.6002	19.928	0.7564	1.163
A21N	8.350E+07	2.093E−03	5.987	0.6269	19.347	0.7550	1.323
B712	6.424E+07	2.171E−03	4.887	0.5910	16.067	0.7020	1.258
B722	8.074E+07	2.103E−03	4.291	0.4992	15.441	0.7738	1.099
B732	6.286E+07	2.178E−03	3.886	0.5567	15.772	0.7036	1.189
B733	6.698E+07	2.158E−03	4.345	0.5782	15.280	0.7322	1.199
B734	7.457E+07	2.126E−03	4.387	0.5766	15.646	0.7309	1.334
B735	6.903E+07	2.149E−03	4.299	0.5502	16.163	0.7322	1.225
B736	6.397E+07	2.172E−03	5.551	0.5638	18.505	0.7613	0.997
B737	6.794E+07	2.154E−03	5.309	0.5677	18.315	0.7613	1.058
B738	7.476E+07	2.125E−03	5.283	0.5817	17.660	0.7613	1.165
B739	8.061E+07	2.103E−03	5.305	0.5825	18.073	0.7597	1.258
B37M	7.737E+07	2.115E−03	6.193	0.5731	19.066	0.7671	1.209
B38M	7.850E+07	2.111E−03	6.108	0.5814	18.674	0.7671	1.227
B39M	8.194E+07	2.098E−03	6.142	0.5964	18.433	0.7655	1.283
B3XM	8.281E+07	2.095E−03	6.093	0.5998	18.284	0.7656	1.297
B742	2.075E+08	1.842E−03	5.727	0.4559	18.032	0.8131	1.495
B743	2.133E+08	1.835E−03	5.772	0.4505	18.241	0.8132	1.536
B744	2.110E+08	1.838E−03	6.438	0.4626	19.349	0.8130	1.469
B748	2.238E+08	1.823E−03	7.347	0.4552	20.793	0.8330	1.459
B752	1.001E+08	2.040E−03	5.730	0.4965	18.048	0.7759	1.242
B753	1.036E+08	2.031E−03	5.628	0.5195	17.348	0.7743	1.288
B762	1.292E+08	1.969E−03	6.278	0.4977	18.746	0.7744	1.312
B763/300ER	1.211E+08	1.987E−03	6.387	0.4696	19.849	0.7758	1.227
B764	1.352E+08	1.956E−03	6.537	0.5414	19.910	0.7746	1.373

https://doi.org/10.1017/aer.2026.10264 Published online by Cambridge University Press

Table 3. *Continued*

ICAO	$A_{1.0}$	$B_{1.0}$	$C_{1.0}$	$E_{1.0}$	$F_{1.0}$	$G_{1.0}$	$H_{1.0}$
B77L	1.868E+08	1.870E−03	7.692	0.5169	22.182	0.8136	1.469
B772	1.619E+08	1.907E−03	6.885	0.4928	20.839	0.8130	1.275
B77W	1.812E+08	1.878E−03	7.303	0.5391	20.885	0.8135	1.426
B773	1.625E+08	1.906E−03	7.091	0.5122	19.724	0.8130	1.280
B788	1.317E+08	1.963E−03	7.783	0.5085	21.697	0.8195	1.096
B789	1.466E+08	1.934E−03	7.793	0.5089	21.697	0.8197	1.220
B78X	1.456E+08	1.936E−03	7.496	0.5129	21.429	0.8195	1.211
C919S	7.085E+07	2.141E−03	12.591	0.5804	19.127	0.7564	1.098
C919L	7.466E+07	2.126E−03	12.604	0.5786	19.211	0.7564	1.157
E75S	5.091E+07	2.243E−03	4.149	0.5526	16.549	0.7366	1.004
E75L	5.054E+07	2.245E−03	4.109	0.5566	16.382	0.7366	0.997
E135	3.284E+07	2.385E−03	3.660	0.5623	15.452	0.7079	0.858
E145	3.564E+07	2.358E−03	3.846	0.5700	15.142	0.7079	0.931
E170	4.621E+07	2.273E−03	4.309	0.5989	17.175	0.7370	0.973
E190	5.325E+07	2.229E−03	4.979	0.5945	17.845	0.7613	0.998
E195	5.336E+07	2.228E−03	4.743	0.5839	16.995	0.7613	0.964
E290	5.709E+07	2.207E−03	5.995	0.5782	20.132	0.7618	0.946
E295	5.864E+07	2.199E−03	5.848	0.6139	19.973	0.7617	0.972
MD82	6.748E+07	2.156E−03	4.566	0.6129	16.554	0.7236	1.165
MD83	7.165E+07	2.138E−03	4.463	0.6192	16.686	0.7219	1.240
GLF5	4.765E+07	2.264E−03	5.968	0.5082	17.595	0.7758	0.791
CRJ9	5.185E+07	2.237E−03	4.434	0.5502	16.279	0.7564	1.092
DC93	5.700E+07	2.208E−03	4.044	0.5654	16.745	0.7370	1.062
RJ1H	5.688E+07	2.208E−03	3.448	0.6343	15.182	0.6520	1.314

decreasing, this is not the case in the example of the real atmosphere shown. The corresponding variations of ΔT and Γ are given in Table 4. In this case, the deviations in static temperature are quite small. However, the deviations in lapse rate are very large and include changes in sign.

Using the twin-aisle aircraft, the variations of optimum Mach number, FL and ($\eta_o L/D$) with aircraft mass are given in Figures 8, 9 and 10. Results are presented for both the observed temperature distribution and the ISA.

The difference between M_{OO} with aircraft mass for the two atmospheres is small, with a maximum of about 1%, but not insignificant in operational terms. However, the important thing to notice is that, whilst the relationship is mostly single-valued, from a mass ratio between 0.675 and 0.690, it is double-valued, and between 0.665 and 0.675, it is triple-valued.

In the case of FL_{OO}, the general trend of increasing FL with decreasing aircraft mass is found. Between the two atmospheres FL differences of up to 10 points, or about 1000 feet, are found and, again, there are double and triple values. These differences, whilst not large, are still operationally significant, particularly in the context of contrail avoidance by changes in altitude.

Figure 10 shows that the variation of the range parameter with mass is also operationally significant, with a change of about 3%. In this example, the impact of atmospheric variation is also significant, with maximum differences being in the region of 1%.

6.0 Improved range equation

The example given in the previous section shows how ($\eta_o L/D$) varies with both aircraft mass, m, and the atmospheric characteristics. This can now be used to estimate the amount of fuel required to cruise a given distance.

https://doi.org/10.1017/aer.2026.10264 Published online by Cambridge University Press

https://doi.org/10.1017/aer.2026.10264 Published online by Cambridge University Press

Table 4. *An example of an observed variation of atmospheric temperature with pressure and the processing steps to estimate steps Γ, Poll and Schumann [9]*

p_∞ (Pa)	T_∞ (K)	FL	ι	dT_∞/dFL (K)	$(T_\infty)_{ISA}$ (K)	ΔT (K)	$\overline{\Delta T}$	LR	Γ_{exact}	Γ_{est}	% diff
26201	222.33	330	0.74505	−0.176	222.77	−0.44	−0.0021	−8.12E−04	−0.225	−0.225	0.0
25594	221.45	335	0.74505	−0.176	221.78	−0.33	−0.0015	−8.12E−04	−0.225	−0.225	−0.1
24999	220.57	340	0.74505	−0.176	220.79	−0.22	−0.0010	−8.12E−04	−0.226	−0.225	−0.2
24415	219.69	345	0.74505	−0.176	219.80	−0.11	−0.0005	−8.12E−04	−0.226	−0.225	−0.2
23842	218.81	350	0.74505	0.802	218.81	0.00	0.0000	3.70E−03	1.025	1.025	0.0
23280	222.82	355	0.74505	0.802	217.82	5.00	0.0231	3.70E−03	1.002	1.001	−0.1
22729	226.83	360	0.74505	−0.018	216.83	10.00	0.0462	−8.17E−05	−0.022	−0.022	0.1
22190	226.74	365	1.00000	−0.018	216.65	10.09	0.0466	−8.12E−05	−0.022	−0.021	−0.5
21663	226.65	370	1.00000	−0.500	216.65	10.00	0.0462	−2.31E−03	−0.610	−0.610	−0.1
21148	224.15	375	1.00000	−0.500	216.65	7.50	0.0346	−2.31E−03	−0.617	−0.617	0.0
20646	221.65	380	1.00000	−0.300	216.65	5.00	0.0231	−1.38E−03	−0.376	−0.375	−0.3
20156	220.15	385	1.00000	−0.300	216.65	3.50	0.0162	−1.38E−03	−0.378	−0.377	−0.3
19677	218.65	390	1.00000	0.100	216.65	2.00	0.0092	4.62E−04	0.127	0.127	−0.3
19210	219.15	395	1.00000	0.100	216.65	2.50	0.0115	4.62E−04	0.127	0.126	−0.3
18754	219.65	400	1.00000	0.100	216.65	3.00	0.0138	4.62E−04	0.127	0.126	−0.3

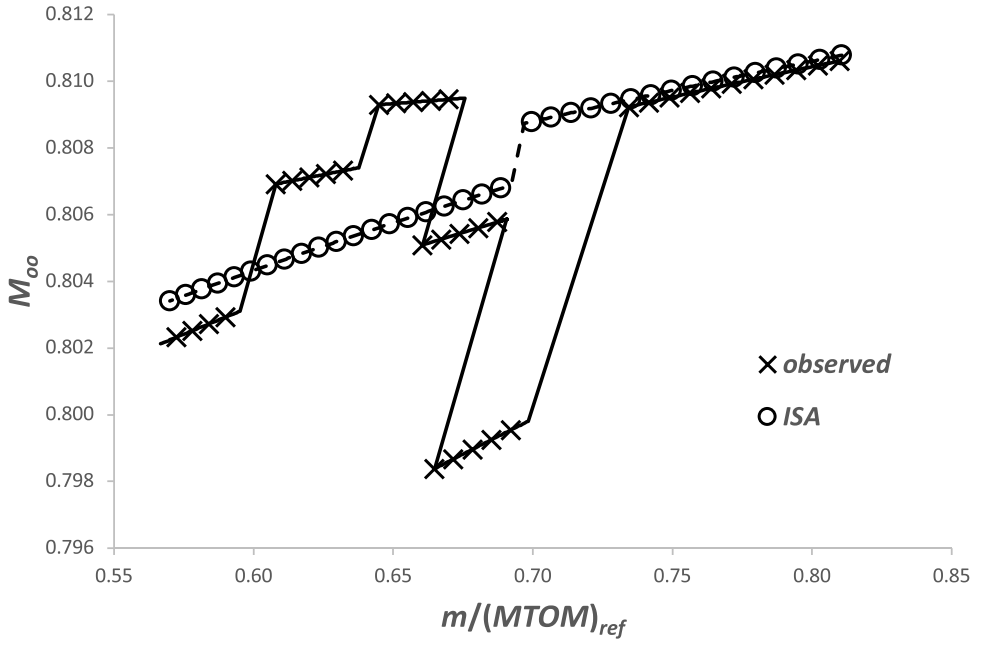


Figure 8. *The variation of the optimum operational FL with aircraft mass for a twin-aisle aircraft.*

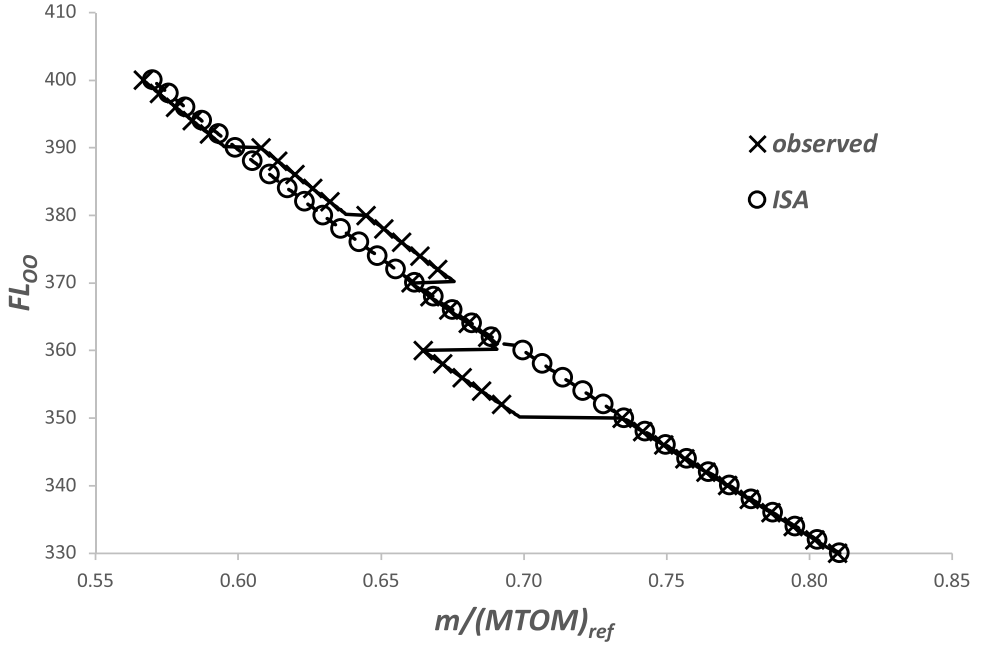


Figure 9. *The variation of the optimum operational FL with aircraft mass for a twin-aisle aircraft.*

The relationship between fuel used and distance travelled through the air in straight and level flight is obtained by rearranging Equation (3) and integrating to give

$$\int_{S_1}^{S_2} dS = \left(\frac{LCV}{g}\right) \int_{m_2}^{m_1} \frac{(\eta_O L/D)}{m} dm \tag{87}$$

https://doi.org/10.1017/aer.2026.10264 Published online by Cambridge University Press

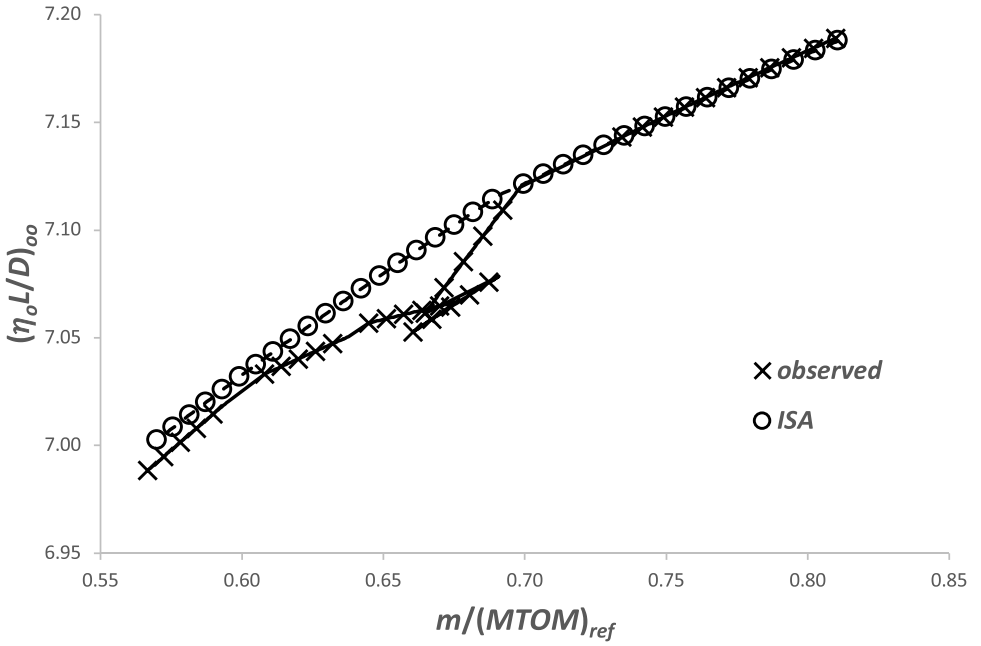


Figure 10. *The variation of the optimum operational range parameter with aircraft mass for a twin-aisle aircraft.*

where m_1 and m_2 are the values of aircraft mass at S_1 and S_2. The difference between m_1 and m_2 is the total fuel used, m_f.

However, wind and temperature data are given in terms of position relative to the ground. Therefore, if there is a tailwind component, V_w, the relationship between S and the distance travelled over the ground, S_G, is

$$\int_{S_1}^{S_2} dS = \int_0^{R_G} \frac{dS_G}{\left(1 + \frac{V_w}{V_\infty}\right)} = R_G - \int_0^{R_G} \frac{V_w}{(V_\infty + V_w)} dS_G = R_G - (\Delta R_G)_w \tag{88}$$

where R_G is the total ground distance travelled. In general, the wind speed and the true airspeed are functions of both position relative to the ground and altitude. As shown in Sections 4.8 and 4.9, the operational optimum values of FL and V_∞ depend upon the aircraft mass, which, in turn, depends upon the fuel usage. This means that the evaluation of these integrals will usually require iteration.

If the range parameter, $(\eta_o L/D)$, is taken to be constant, the fuel required for a given ground distance is

$$\frac{m_f}{m_1} = 1 - EXP\left(-\frac{(R_G - (\Delta R_G)_w)\,.g}{(\eta_o L/D)\,LCV}\right) \tag{89}$$

This is a version of the well-known Breguet range equation inverted to give mission fuel as a function of range (see, for example, Torenbeek [5], Martinez-Val et al. [6] and Randle et al. [7]).

However, as shown in Section 2.5, the range parameter is a function of the aircraft mass, with the general form being

$$(\eta_o L/D)_{OO} \propto \left(\frac{m}{MTOM_{ref}}\right)^{\epsilon} \tag{90}$$

and, as shown in Section 2.5, if m is greater than, or equal to, m_T (Equation (60), or (61)), ε is equal to 0.063 ± 0.0025 (Equation 65) and if m is less than m_T, ε is equal to 0.083 ± 0.0035 (Equation (66)).

https://doi.org/10.1017/aer.2026.10264 Published online by Cambridge University Press

Hence, from Equation (87), if m is always greater than m_T,

$$\int_{S_1}^{S_2} \frac{dS}{(1-0.11(\overline{\Delta T})_{OO})} = 15.87\left(\frac{(\eta_O L/D)_{m_1}.LCV}{g\left(1-0.11(\overline{\Delta T})_{OO}^{S_1}\right)}\right)\left(1-\left(\frac{m_2}{m_1}\right)^{0.063}\right) \tag{91}$$

Now, using the results in Equation (88),

$$\int_{S_1}^{S_2} \frac{dS}{(1-0.11(\overline{\Delta T})_{OO})} \approx \int_0^{R_G} \frac{V_\infty\left(1+0.11(\overline{\Delta T})_{OO}\right)}{(V_\infty+V_w)} dS_G = R_G - (\Delta R_G)_w + (\Delta R_G)_{\Delta T} \tag{92}$$

where

$$(\Delta R_G)_{\Delta T} \approx 0.11\int_0^{R_G} \frac{V_\infty(\overline{\Delta T})_{OO}}{(V_\infty+V_w)} dS_G \tag{93}$$

In general, and to maintain $(\eta_o L/D)$ at its optimum value, the aircraft will be changing altitude as S_G as increases. Consequently, this term involves changes in tailwind and temperature in both the horizontal and vertical planes. Therefore, as with $(\Delta R_G)_W$, evaluation of $(\Delta R_G)_{\Delta T}$ will require iteration.

The corresponding fuel requirement is

$$\frac{m_f}{m_1} = 1-\left(1-0.063\left(\frac{g\left(1-0.11(\overline{\Delta T})_{OO}^{S_1}\right)}{(\eta_O L/D)_{m_1} LCV}\left(R_G-(\Delta R_G)_w+(\Delta R_G)_{\Delta T}\right)\right)\right)^{15.87} \tag{94}$$

Similarly, if m is always less than m_T,

$$\frac{m_f}{m_1} = 1-\left(1-0.083\left(\frac{g\left(1-0.11(\overline{\Delta T})_{OO}^{S_1}\right)}{(\eta_O L/D)_{m_1} LCV}\left(R_G-(\Delta R_G)_w+(\Delta R_G)_{\Delta T}\right)\right)\right)^{12.05} \tag{95}$$

In the special case where m_2 is equal to m_T, the ground distance covered is

$$(R_G-(\Delta R_G)_w+(\Delta R_G)_{\Delta T})_T = (R_G)_T - \int_0^{(R_G)_T} \frac{V_w}{(V_\infty+V_w)} dS_G + 0.11\int_0^{(R_G)_T} \frac{V_\infty(\overline{\Delta T})_{OO}}{(V_\infty+V_w)} dS_G \tag{96}$$

and

$$(R_G)_T \approx 15.87\left(\frac{\left(\frac{\eta_O L}{D}\right)_{m_1}.LCV}{g\left(1-0.11(\overline{\Delta T})_{OO}^{S_1}\right)}\right)\left(1-\left(\frac{m_T}{m_1}\right)^{0.063}\right)+((\Delta R_G)_w-(\Delta R_G)_{\Delta T})_T \tag{97}$$

whilst the fuel used is

$$\frac{(m_f)_T}{m_1} = 1-\frac{m_T}{m_1} \tag{98}$$

Hence, if m_1 is greater than m_T and m_2 is less than m_T, the fuel requirement is

$$\frac{m_f}{m_T} = 1-\frac{m_T}{m_1}\left(1-0.083\left(\frac{g\left(1-0.11(\overline{\Delta T})_{OO}^{(R_G)_T}\right)}{(\eta_O L/D)_{m_T} LCV}\left(R_G-(R_G)_T-[(\Delta R_G)_w-(\Delta R_G)_{\Delta T}]_{(R_G)_T}^{R_G}\right)\right)\right)^{12.05} \tag{99}$$

7.0 Discussion

Although the foregoing analysis may appear to be complex, the results given in Sections 4.2 to 4.9 are both simple and easy to use. The operational optimum range parameter, $(\eta_o L/D)_{OO}$, is found to have a clear dependency upon aircraft mass, increasing as the mass increases. For take-off masses ranging from the minimum likely to the maximum possible, the difference is about 5%. This is large enough to affect the trip fuel requirement for long-haul flights where weight loss due to fuel may be up to 25% of the take-off value. Deviations in atmospheric static temperature from the ISA values also have a noticeable

https://doi.org/10.1017/aer.2026.10264 Published online by Cambridge University Press

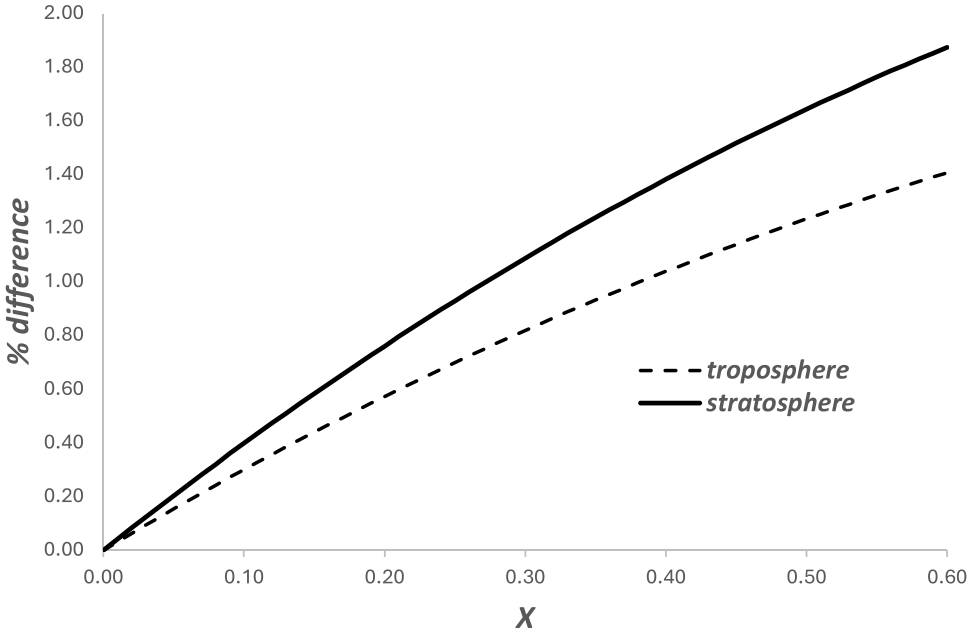


Figure 11. *A comparison between the improved range equations and the Breguet version for ISA conditions and zero wind with total distance flown.*

effect, with $(\eta_o L/D)$ decreasing as ΔT increases, again, changes of the order$\pm$1% are possible. However, variations in the vertical temperature lapse rate (LR) are found to be negligible.

The optimum value of lift coefficient is a very weak function of mass and is independent of ΔT. However, it does depend upon LR, with changes of $\pm$2% being possible. In addition, the optimum Mach number, which was assumed to be constant in previous work, is found to exhibit a weak dependence upon m, ΔT and LR. In all cases, the maximum likely variation is of order$\pm$1%. The optimum FL depends upon the optimum values of both lift coefficient and Mach number. Whilst the FL is driven primarily by aircraft mass, increases in ΔT can reduce the optimum FL by about 2 units ($\approx$200 feet), whilst increases in LR can reduce it by 8 units ($\approx$800 feet).

The results obtained in this analysis are both qualitatively and quantitatively similar to those presented in the original papers by Poll and Schumann [9, 10]. In this case, a much simpler model, proposed by Poll [8], was used to represent the aircraft and engine combination. This was based upon the hypothesis that, when suitably normalised, the variation of $(\eta_o L/D)$ with Mach number and lift coefficient was approximately the same for all aircraft. The results of the present study provide evidence in support of that very simple hypothesis.

Regarding the extended range equation, Figure 11 gives the results from Equations (94) and (95) compared with those from the Breguet equation, Equation (89), for zero wind and ISA conditions. In this particular case, the impact of varying aircraft mass as fuel is consumed is shown, and the non-dimensional ground distance flown is

$$X = \frac{g.R_G}{(\eta_O L/D)_{m_1}\, LCV} \tag{100}$$

The upper limit of X equal to 0.6 corresponds to a range of about 20,000 *kms*, or half the circumference of the Earth. A trip from London to Johannesburg is about 10,000 *kms*, i.e. an X of about 0.3, whilst London to New York is about 5,000 *kms*, or an X of approximately 0.15. The classic Breguet equation always gives a lower value of (m_f/m_1) for a given X and, whilst these differences are not large, being around 1% for long-haul flights. This is equivalent to about 1,000 *kgs* of fuel. It is also important

https://doi.org/10.1017/aer.2026.10264 Published online by Cambridge University Press

to note that assuming ($\eta_o L/D$) to be fixed at its initial value locks out the effect of en-route temperature variations, and these may also change the fuel requirement by a similar amount.

Finally, in the example described in Section 5.0, it was found that, for some values of mass, there were multiple solutions for the optimum FL and Mach number. This is because, unlike the ISA, the variation of temperature with pressure is not a monotonically decreasing (or increasing) function. Specifically, referring to Figures 8 and 9, for masses in the range 0.665–0.675, there are three solutions for FL_{OO} ranging from 360 to 375, i.e. a 4% change. Similarly, there are three values of M_{OO} ranging from 0.798 ($FL_{OO} = 360$) to 0.810 ($FL_{OO} = 360$), i.e. 1.5%. However, as shown in Figure 10, the range parameter and, hence, the SAR is essentially constant. Therefore, in this example, the operator would have a choice of three different FLs for the same SAR and with Mach numbers differing only by about 1%. This has important implications for planning flights that avoid contrails by flying above, or below, regions of the atmosphere where the air is super-saturated with respect to ice.

Any desk-based study for flight in the ISA would find a single solution for the operating conditions at each aircraft mass. Consequently, moving away from the optimum FL to avoid an ISSR would necessarily incur a small fuel penalty. However, as shown above, this is not a conclusion that is valid for all atmospheric conditions; rather, it is a specific result valid only for the idealised ISA.

8.0 Conclusions

Previous work has been extended to provide rapid and accurate estimates of the optimum operational SAR for an aircraft of given total mass in a completely general atmosphere. Simple relationships have also been found for the corresponding values of lift coefficient, Mach number and FL. The variation of optimum operational SAR with mass is significant, and it increases as the aircraft mass increases. In addition, there is a small reduction in SAR as the air temperature increases above the ISA value for the same FL. Taking these influences into account, an improved and complete range equation, including the effects of wind and temperature variations in both the horizontal and vertical wind planes, has been presented. Depending upon the distance flown and the atmospheric conditions en route, the trip fuel requirement may vary by several percent relative to the estimates from the traditional Breguet formulation.

The FL for optimum SAR is found to depend upon both the local temperature deviation from ISA and the vertical temperature lapse rate. Sample calculations using an observed temperature profile show that, in regions where the sign of the lapse rate is changing, there can be more than one solution for the FL for optimum SAR for a given aircraft mass. The possibility that very nearly the same value of SAR may be achieved at more than one FL has implications for fuel usage when exercising contrail avoidance by vertical deviation. Currently, there is a widely held belief that any (temporary) deviation in cruise altitude from an aircraft's flight-plan value must lead to an increase in fuel consumption. This may be true for operation in the idealised ISA. However, since changes in SAR with height in the real atmosphere may differ significantly in magnitude and may be of opposite sign to those occurring in the ISA, when avoiding contrails, it may be possible to move to different altitudes at which the SAR is essentially the same as the undisturbed, flight-plan value and, possibly, even less. To ensure continuous operation at optimum, or near optimum, conditions, accurate temperature and temperature gradient data are required all along the route and in real time.

Airlines operate their aircraft using a cost index, which is the ratio of the cost of time to the cost of fuel for a flight. Conditions for optimum SAR correspond to operation at a cost index of zero. This method provides a baseline for future work exploring the implications of operating at a non-zero cost index.

Disclaimer. The values of the coefficients given in this paper are based solely upon information that is available in the public domain. Since the absolute accuracy of such data cannot be guaranteed, the numbers should be treated as 'best estimates' and, as such, may be subject to some error.

https://doi.org/10.1017/aer.2026.10264 Published online by Cambridge University Press

References

[1] ICAO. *Manual of the ICAO Standard Atmosphere. ICAO Document No. 7488, 2nd Edition,* 1964.

[2] Poll, D.I.A. and Schumann, U. On the conditions for absolute minimum fuel burn for turbofan powered, civil transport aircraft and a simple model for wave drag, *Aeronaut. J.*, 2024, **128**, pp 1071–1103. https://doi.org/10.1017/aer.2024.10.

[3] Poll, D.I.A. and Schumann, U. A simple model for the estimation of turbofan engine performance in all airborne phases of flight, *Aeronaut. J.*, 2024, **128**, pp 2725–2753. https://doi.org/10.1017/aer.2024.92.

[4] Poll, D.I.A. and Schumann, U. An estimation method for the fuel burn and other performance characteristics of civil transport aircraft: Part 3 full flight profile when the trajectory is specified, *Aeronaut. J.*, 2025, **129**, pp 825–861. https://doi.org/10.1017/aer.2024.141.

[5] Torenbeek, E. *Advanced Aircraft Design – Conceptual Design, Analysis and Optimisation of Subsonic Civil Aeroplanes*, John Wiley and Sons, 2013, Chichester, West Sussex, UK, ISBN: 9781119969303.

[6] Martinez-Val, R., Palacin, J.F. and Perez, E. The evolution of jet airliners explained through the range equation, *Proc. Inst. Mech. Eng. Part G: J. Aerosp. Eng.*, 2008, **222**, pp 915–919. https://doi.org/10.1243/09544100JAERO338.

[7] Randle, W.E., Hall, C.A. and Vera-Morales, M. Improved range equation based on aircraft data, *J. Aircraft.*, 2011, **48**, pp 1291–1298. https://doi.org/10.2514/1.C031262

[8] Poll, D.I.A. On the relationship between non-optimum operations and fuel requirement for large civil transport aircraft, with reference to environmental impact and contrail avoidance strategy, *Aeronaut. J.*, 2018, **122**, pp 1827–1870. https://doi.org/10.1017/aer.2018.121.

[9] Poll, D.I.A. and Schumann, U. An estimation method for the fuel burn and other performance characteristics of civil transport aircraft in the cruise. Part 1 fundamental quantities and governing relations for a general atmosphere, *Aeronaut. J.*, 2021, **125**, pp 257–295. https://doi.org/10.1017/aer.2020.62.

[10] Poll, D.I.A. and Schumann, U. An estimation method for the fuel burn and other performance characteristics of civil transport aircraft in the cruise. Part 2 determining the aircraft's characteristic parameters, *Aeronaut. J.*, 2021, **125**, pp 296–340. https://doi.org/10.1017/aer.2020.124.

Appendix A. Approximate relations for Reynolds number and Γ

Starting with the definition of Reynolds number given in Equation (10)

$$R^{ac} = S_{ref}^{1/2}\left(\frac{\gamma p_{TP}}{\mu_{TP}a_{TP}}\right)_{ISA}\left(\frac{(\mu_{TP}a_{TP})_{ISA}}{\mu_\infty a_\infty}\right)\left(\frac{p_\infty}{(p_{TP})_{ISA}}\right)M_\infty = \frac{\psi_5}{\phi}\left(\frac{p_\infty}{(p_{TP})_{ISA}}\right)M_\infty \tag{A1}$$

Here the temperature dependent quantities are confined to the term ϕ and ϕ is a function of temperature alone. For temperatures in the range 175 K to 265 K, it is shown in Poll and Schumann [9] that ϕ may be represented by the power law

$$\frac{\mu_\infty a_\infty}{(\mu_{TP}a_{TP})_{ISA}} = \phi \approx \left(\frac{T_\infty}{(T_{TP})_{ISA}}\right)^{1.34} \tag{A2}$$

to an accuracy of better than ±0.5%. Hence,

$$\frac{T_\infty}{\phi}\frac{d\phi}{dT_\infty} \approx 1.34 \tag{A3}$$

which is accurate to better than ±3.5% over the same range.

If the static temperature, T_∞, in a general atmosphere is written as $(T_\infty)_{ISA}$ plus ΔT, where ΔT is a function of FL and is generally small compared to $(T_\infty)_{ISA}$, then

$$\frac{T_\infty}{(T_{TP})_{ISA}} = \left(\frac{T_\infty}{T_{TP}}\right)_{ISA} + \frac{\Delta T}{(T_{TP})_{ISA}} = \overline{T} + \overline{\Delta T} \tag{A4}$$

Hence,

$$\phi \approx \left(1 + 1.34\frac{\overline{\Delta T}}{\overline{T}}\right)\overline{T}^{1.34} \tag{A5}$$

and, in the vicinity of the 226.32 *hPa* isobar (ISA tropopause) where $\overline{T}$ is close to unity, the simplified expression,

$$\phi \approx (1 + 1.34\overline{\Delta T})\overline{T}^{1.34} \tag{A6}$$

https://doi.org/10.1017/aer.2026.10264 Published online by Cambridge University Press

may be used. For attitudes above 28,000 feet, Equation (A6) is found to be accurate to better than ±2% for values of $\overline{\Delta T}$ in the range ±0.15.

In a general atmosphere, temperature, pressure and altitude are linked by the hydrostatic equation, i.e.

$$dp_\infty = -\rho_\infty g_{SL} dh = -\left(\frac{30.48 g_{SL}}{\Re}\right)\left(\frac{p_\infty}{T_\infty}\right) dFL \tag{A7}$$

where ρ_∞ is the local air density and g_{SL} is the acceleration due to gravity at sea level. Hence, for the ISA,

$$\overline{T} = \left(\frac{(p_{TP})_{ISA}}{p_\infty}\right)^{\omega} \tag{A8}$$

where the exponent ω is a constant given by

$$\omega = \frac{\Re L_h}{g_{SL}} \tag{A9}$$

and $\Re$ is the gas constant for air. Therefore,

$$\phi \approx \left(1 + 1.34\overline{\Delta T}\right)\left(\frac{(p_{TP})_{ISA}}{p_\infty}\right)^{1.34\omega} \tag{A10}$$

and

$$R^{ac} = \psi_5 \left(\frac{p_\infty}{(p_{TP})_{ISA}}\right)^{\iota}\left(\frac{M_\infty}{1 + 1.34\overline{\Delta T}}\right) \tag{A11}$$

where

$$\iota = 1 + 1.34\omega \tag{A12}$$

In the ISA [1], the troposphere and the stratosphere are regions within which the local, vertical temperature gradient, or 'lapse' rate, is constant. This gradient is expressed as the derivative of temperature with respect to the geopotential altitude[8], h, designated here as L_h and which has units of *K/m*. When p_∞ is greater than, or equal to, $(p_{TP})_{ISA}$, L_h is −0.0065 *K/m*, ω is –0.19026 and i is 0.74505, otherwise, both L_h and ω are zero, i is equal to one.

As also described in Poll and Schumann [9]

$$\Gamma = -\frac{p_\infty}{\phi}\frac{d\phi}{dp_\infty} \tag{A13}$$

When FLs are used to define altitude the variation of dp_∞/dFL with FL is the same in all atmospheres and from Equation (A7),

$$\left(\frac{p_\infty}{FL}\frac{dFL}{dp_\infty}\right) = \left(\frac{p_\infty}{FL}\frac{dFL}{dp_\infty}\right)_{ISA} = -\left(\frac{\Re(T_{TP})_{ISA}}{30.48 g_{SL}}\right)\left(\frac{\overline{T}}{FL}\right) = -208.06\left(\frac{\overline{T}}{FL}\right) \tag{A14}$$

However, the variation of temperature with pressure and, hence, the variation of dT_∞/dFL with FL depend upon the actual atmospheric conditions. Therefore, in general, using Equations (A3) and (A14),

$$\Gamma = -\left(\frac{T_\infty}{\phi}\frac{d\phi}{dT_\infty}\right)\left(\frac{p_\infty}{FL}\frac{dFL}{dp_\infty}\right)\left(\frac{FL}{T_\infty}\frac{dT_\infty}{dFL}\right) \approx 278.8\left(\frac{\overline{T}}{FL}\right)\left(\frac{FL}{T_\infty}\frac{dT_\infty}{dFL}\right) \tag{A15}$$

and, from Equation (A4),

$$\left(\frac{FL}{T_\infty}\frac{dT_\infty}{dFL}\right) = \frac{FL}{\left(\overline{T} + \overline{\Delta T}\right)}\left(\frac{d\left(\overline{T} + \overline{\Delta T}\right)}{dFL}\right) = \frac{\overline{T}}{\left(\overline{T} + \overline{\Delta T}\right)}\left(\frac{FL}{\overline{T}}\right)\frac{1}{(T_{TP})_{ISA}}\frac{dT_\infty}{dFL} \tag{A16}$$

[8] The geopotential altitude is the gravitational potential energy per unit mass at a given geometric altitude, measured relative to mean sea level, divided by the acceleration due to gravity at sea level.

https://doi.org/10.1017/aer.2026.10264 Published online by Cambridge University Press

Hence,

$$\Gamma \approx 278.8 \left(\frac{\overline{T}}{\overline{T} + \overline{\Delta T}} \right) LR \tag{A17}$$

where LR is the non-dimensional, temperature change per FL defined as

$$LR = \frac{1}{(T_{TP})_{ISA}} \frac{dT_\infty}{dFL} = 0.1407 L_h \tag{A18}$$

This result is valid for all FLs. However, in the vicinity of FL 360, where $\overline{T}$ is close to unity,

$$\Gamma \approx 277(1 - \overline{\Delta T}) LR \tag{A19}$$

Here, the constant of proportionality has been adjusted so that, for FLs greater than 280, this expression is accurate to better than ±3.5%, when $\overline{\Delta T}$ and LR are in the range ±0.15 and ±0.0045 respectively.

Cite this article: Poll D.I.A. and Schumann U. Optimum fuel use for turbofan-powered aircraft in a completely general atmosphere with an improved range equation. *The Aeronautical Journal*, https://doi.org/10.1017/aer.2026.10264

https://doi.org/10.1017/aer.2026.10264 Published online by Cambridge University Press